THE UNIVERSITY *of* LIVERPOOL

ADVANCED WINDING MODELS AND ONTOLOGY-BASED FAULT DIAGNOSIS FOR POWER TRANSFORMERS

Thesis submitted in accordance with the
requirements of the University of Liverpool
for the degree of Master of Philosophy

in

Electrical Engineering and Electronics

by

CHEN LU, B.Sc.(Eng.)

July 2014

ADVANCED WINDING MODELS AND ONTOLOGY-BASED FAULT DIAGNOSIS FOR POWER TRANSFORMERS

by

CHEN LU

Acknowledgements

I would like to give my heartfelt thanks to my supervisor, Dr. T. T. Mu, whose encouragement, guidance and support enabled me to develop a deep understanding of my work. Her intellectual advice, encouragement and invaluable discussions were the driving force in my work and have deeply broadened my knowledge in many areas, for which I am truly grateful.

Many thanks to Prof. Q. H. Wu and Dr. W. H. Tang, for their professional guidance. Their drive, enthusiasm, their hard work and knowledge that has triggered and nourished my intellectual maturity.

I offer my regards and blessings to all of the members of Electrical Drives, Power and Control Research Group, the University of Liverpool, especially to Dr. L. Jiang, Dr. W. Yao, Dr. J. D. Jin, Mr. C. H. Wei, Mr. L. Yan and Mr. L. Zhu. Special thanks also go to my friends, J. Chen, Z. Wang, for their support and friendship. My thanks also go to the Department of Electrical Engineering and Electronics at the University of Liverpool, for providing the research facilities that made it possible for me to carry out this research.

Last but not least, my thanks go to my beloved family for their loving considerations and great confidence in me through these years.

Abstract

Power transformer plays an important role in a power system, and its fault diagnosis has been recognised as a matter of most considerable interest in maintaining the reliable operation of a power system. In practise, operation and fault diagnosis of the power transformer are based on knowledge and experience of electrical power engineers. There are several on-line diagnosis methods to monitor the power transformer, such as dissolved gasses analysis (DGA), partial discharge (PD), and frequency response analysis (FRA). In order to reduce the cost and increase fault diagnosis efficiency, new techniques and expert-systems are required, which can provide power transformer failure knowledge representation, automated data analysis and decision-making.

Power transformer failure modes and diagnostic methods have been reviewed in Chapter 1. Then, ontology has been employed in establishing the power failure models system. Ontology is a mechanism that describes the concepts and their systematic relationships. In order to develop ontology system for the power failure models system, numerous concepts and their relationships between faults exhibited for power transformers are analysed. This system uses a software called $Protégé$, which is based on ontology to provide a semantic model for knowledge representation and information management. The relationship between electrical failure models has been illustrated successfully, and the system can correctly provide a query searching function.

Partial discharge (PD) is a common fault in power transformer, it may causes gradual degradation of power transformer insulation material, which may finally lead to a full break down. Localisation of PD source is vital for saving in maintenance time and costs, but it is not a simple task in application due to noise signal

and interference. The multi-conductor transmission model (MTL) is one of the most suitable models for PD propagation study in transformers. Chapter 3 shows an initial study of MTL model and tests its effectiveness of PD faults locations. Then, the transfer function from all possible PD locations to line-end and neutral-end were calculated. The results proved that this method can estimate the location of PD very effectively.

FRA is a diagnosis method for detecting winding deformation based on variation of power transformer AC impedance. In chapter 4, a lumped parameter winding model of single phase power transformer is introduced. However, the FRA frequency range of original lumped model is only available up to 1MHz. In order to improve frequency response range, an advanced lumped model has been proposed by adding a negative-value capacitive branch with inductance branch in the original model. It significantly enhances the valid range of frequency up to 3MHz.

In chapter 5, three optimisation methods, particle swarm optimisation (PSO), genetic algorithms (GA), and simulated annealing (SA) are subsequently applied for transformer parameter identification based on FRA measurements. The simulation results show that PSO, GA, and SA can accurately identify the parameters, partial significance of the deviation between simulation with reference is acceptable. The model with the optimised parameters ideally describes the magnetic and electrical characteristics of the given transformer. The comparison of results from the optimisation methods shows that converge time of PSO is shorter than others' and the GA provides the best FRA outputs, which is more closer to reference in a limited number of iterations.

Declaration

The author hereby declares that this thesis is a record of work carried out in the Department of Electrical Engineering and Electronics at the University of Liverpool during the period from October 2011 to July 2014. The thesis is original in content except where otherwise indicated.

Contents

List of Figures

List of Tables

Chapter 1

Introduction

1.1 Motivation

Power transformer is one key equipment in a power system, and plays many important roles in the system, whose functions include converting the level of a voltage or current, separation of the system into several subsystems which decreases the apparent value of capacitors, inductors and resistances applied. Moreover, the transformer is used for high-voltage long distance electrical energy transmission purposes as well as for low-voltage energy distribution to end consumers. Ensuring the transformer is under good operation condition, can provide the following benefits to the power system, such as high reliability, high efficiency, and reduction of the financial costing. Since the transformer can operate for a long period of time up to 50 years, failures and accident cannot be avoided during its operation period. There are many reasons that can cause failures and accidents, such as the destruction of the external force, influence of natural disasters, existing in the installation, repair and maintenance issues, and manufacture process faults and other accidents. Moreover, due to the long-term operation the power transformer will generate the degradation of the material and affect the power transformer life cycle, which is the main cause of failure. On the other hand, engineers may not be capable of finding the failures due to non technical diagnostic knowledge, therefore if a small problems cannot be solved in time, which in turn can cause a large accident.

In order to detect the large amount of failure modes, it requires a team of experts in different areas and complicated information should be analysed. Due to complexities of failure and engineer limited knowledge, engineers find it very difficult to identify every transformer failure mode. In order to reduce the human intervention for handling the complex data, a new system is required for knowledge representation, automated data analysis and decision-making.

1.2 Background of Fault Diagnosis for Power Transformer

There are various reasons that can cause transformer failures, such as insulation problems, installation problems, and quality of manufacture, lightning surge and shot periods of overloading. Sometimes transformer failure also can be caused by abnormal operation procedure or lack of maintenance. Therefore, transformer assessment needs to be applied to ensure the highest efficiency and optimum life, which minimises the risk of premature failure and reduces the maintenance costs[14][15].

1.2.1 Faults of Power Transformer

Power transformer faults are generally composed of internal faults and external faults. The most common internal faults are caused by electrical failures in windings and leads, such as short-circuit between turns, short-circuit between strands, and short-circuit to ground. Meanwhile, the reason for external faults is degradation of external insulation, for example, electrical insulator flashover or broken cause grounding. This chapter illustrates electrical failures, mechanical fault, partial discharge failures, and degradation failure fault.

1.2.1.1 Electrical Failure

Electrical failures are classified into two groups: electrical failures in windings and leads, and electrical failures in the core. The most common faults of electrical

failure in windings and leads include short-circuit between turns and short-circuit between strands, and short-circuit to ground.

Short Circuit Between Turns (SCBT)

There are several reasons that can cause SCBT. Firstly, winding deformation, which can lead to axial deformation and vibration, which damages solid insulation between turns followed by a short-circuit fault. The external factors of winding deformation are external short-circuit, out of phase synchronisation, losing clamping structure, axial forces and manufacturing mistake. The effect of short-circuit leads to abnormal temperatures as well as aging by-products such as particles, and gasses. Protection can be achieved by detecting these failures using Buchholz.

Short Circuit Between Strands (SCBS)

SCBS is very similar to the faults mentioned above. Normally, solid insulation mechanical fatigue can cause a short-circuit between strands. It can be caused by either vibration due to axial deformation or internal movement influenced by losing clamping and axial deformation during transportation. Moreover, the dielectric strength of aged cellulose could be reduced during re-clamping which leads to SCBT or SCBS in transformers.

Short Circuit to Ground (SCTG)

Degradation of insulation usually exists in aged transformers. Either degradation of insulation between windings and core or between leads and grounding will lead to SCTG. This failure mode causes overheating and carbonisation in current-carrying elements. The short-circuit can generate overheating eventually burning and turn into an open-circuit.

Besides winding faults, failures in the cores of power transformers have been discussed in previous research. They can be divided into three types short-circuit core laminations, multiple cores grounding, and ungrounded core.

Short Circuited Core Laminations (SCCL)

The abnormal temperature in the core generates a degradation process of the

insulation between laminations. It causes SCCL in the future. The shorted laminations create load components in the exciting current, which increases the temperature and generate gasses, this could cause a trip of the Buchholz relay.

Multiple Core Grounding (MCG)

MCG can lose insulation of the core to ground, which leads to a short circuit to ground. Hence currents circulating through the core, cause local overheating accompanied by gassing.

Ungrounded Core (UC)

There are three factors that can lead to UC: manufacturing mistakes, high contact resistance of the core and externally disconnected core grounding. In order to avoid the influence of circulating currents, a high resistance is applied to the ground in the core of transformers.

According to the statistics of power transformer faults, about 19 % of all occurring emergencies are winding faults [15][16]. However, another survey of 15-25 year old transformers indicates that winding deformation failure accounts for almost 2 out of 3 of all failures.

1.2.1.2 Mechanical Failure

Mechanical failures can be divided into three types: axial deformations, radial deformations, and lead deformations.

Axial deformations are caused by over-current. Over-currents can cause axial forces, radial forces, and opposing forces. Axial forces on clamping rings which leads to axial instability and short-circuit between turns, also axial forces within a given coil group will cause beam stress on the conductors which then lead to conductor bending. Radial forces lead conductors are stretched or compressed then break the conductors to cause open-circuit. Opposing forces directed axially towards the winding centre will cause tilt in conductors so that axial instability occurs. High over currents can be caused by clamping system failures. The main reason for clamping

structure loss are paper shrinkage due to drying, vibrations caused by the normal aging and axial forces caused by short circuit currents.

Radial deformation is caused by external short-circuit currents, such as buckling deformation. Moderate radial deformations can cause the conductor insulation to tear or separate.

Lead deformations are caused by external short-circuit, out of phase synchronization, high inrush current and shocks during transportation. Lead deformation will affect arcing, and flashover.

1.2.1.3 Patrial Discharge

Discharge happens in the insulation structure when inside the air gap, the oil film, occurs at the edges of the conductor. Partial discharge is a low energy discharge. It can cause equipment breakdown or damage. According to the different insulation parts, partial discharge can be divided into the solid insulation discharge, and discharge in the oil. There are many reasons for partial discharge, (1) When there are bubbles in the oil or holes in solid insulating materials. It is easy to cause the discharge in the air gap. (2) The influence of external environmental conditions, the disposal of unclearly oil can cause discharge in the gap. (3) The quality of the transformer is inadequate, some parts may have an angle which will cause a discharge. (4) Poor contact between the metal parts cause partial discharge.

1.2.1.4 Sparking and Arcing

Sparking is a common phenomenon in the power transformer, this is caused by a closed loop between adjacent members linked by stray flux, main flux or by floating potential. Loose clamping can cause arcing/sparking discharges at the clamping bolts/bosses, producing fine carbon contamination everywhere particularly on the top frame surfaces [17]. Also, spark discharge is generated in transformer oil by the impurities in the oil. Arcing is a high-energy discharge, it can breakdown insulation layers in winding turns. It can also causes fracture, flash over and tap-changer fault.

- Arcing influences the change of electronic form to impact dielectrically, leading to perforation of the insulating paper, burning or carbonization, so that the

deformation of metal material and burning can lead to an explosive accident. An accident is difficult to predict in advance whith obvious warning.

- Arcing discharge generates gasses, the gas relay shows the proportion of H_2 and C_2H_2 significantly higher. The main gases in the oil are H_2, C_2H_2, CH_4 and C_2H_6. When discharge failure is involved in solid insulation it also produce CO and CO_2.

1.2.1.5 Degradation Insulation Failure

There are two kinds of power transformers that have widely used around the world, the oil-immersed type transformer and the dry type paper transformer. Different insulation materials of two transformer models are applied. The insulation of oil-immersed transformers include insulation oil, insulation paper, solid insulation paper, cardboard and wood. Degradation of insulation materials are caused by environmental factors, which lead to reduction of performance or loss of the dielectric strength.

Degradation Solid Paper Insulation Fault

Solid paper insulation is one of the main parts of the oil immersed transformer insulation. It includes insulation paper, and insulation board. Its main composition is cellulose. Insulation paper aging reduces the degree of polymerisation and tensile strength, and generates water, CO, CO_2, and furan formaldehyde. These products are harmful to electrical equipment and reduce the ability of insulation paper, such as, loss of dielectric property, reduction of tensile strength, and corrosion of metal materials in the equipment. High quality solid materials should have good electrical and mechanical insulating performance.

Degradation Mechanisms Involving Over-heating

General and local overheating can cause harm to power transformers. There are many factors that can cause overheating, such as cooling deficiency, overloads, poor joints, and circulating currents. Overheating usually generates gasses which degrades the oil insulation and the resulting high temperature

will have an effect on the paper in the solid insulation. Moreover, a possible generation of carbon and other aging-byproducts contribute to further degradation of the insulation fluid. On the other hand, poor joints increase the value of contact resistance, at the same time it will cause oil overheating and local overheating. Local overheating leads to cooking or melting of conductors. Also, local overheating generates gasses which degrade insulation due to the aging of the oil. Local overheating can also be produced by either main flux or stray flux.

Degradation Mechanisms Involving Water and Oil Aging By-Products

Water is a factor in degradation, it exists in three different forms in power transformer, which are free water molecules, steam and bonded-water molecules. Water not only locates in the oil insulation but also in the paper insulation. The characteristics of dielectric parameters of the oil, such as conductivity, permittivity and dissipation factor, are changed by water. Once the parameters of the oil have been modified they can cause breakdown faults. Without the water, the particles can also cause a breakdown of oil. There are different kinds of particles in the transformer such as cellulose fibres, iron, aluminum, copper and others. All these particles are created and reside in the transformer oil. Degradation of dielectric strength of transformer insulation is mainly influenced by particle contamination, and the most harmful particles are conductive mode particles such as metal, carbon, and wet fibres. When the useful life of paper insulation reduces, the production of bubbles in the oil would contribute to the breakdown of oil insulation. Bubbles can also from oil aging products, which lead to degradation of insulation.

Degradation Mechanism Involving Short-circuit between Turns/ Strands

Short-circuit between turns can affect the main magnetic flux. It creates a circulating current, which generates a load component in the measured exciting current and loss. The degraded insulation is caused by generated gases and causes abnormal temperature.

Degradation Mechanism Involving Partial Discharge

Partial discharge (PD) is an electrical discharge that only partially bridges that insulation between conductors or interfaces within the insulating system or from the sharp edges of energized apparatus parts. It may be induced by temporary over-voltage, an incipient weakness in the insulation introduced during manufacturing, or as a result of degradation over the transformer lifetime. Different classes of defects result in PD activity in oil filled power transformers, such as, bad contacts, floating components, suspended particles, protrusions, rolling particles, and surface discharges.

Partial discharges are undesirable because of the possible deterioration of insulation with the formation of ionized gas due to this breakdown that may accumulate at or in a critical stress region. This generally involves non-self-restoring insulation that may be subject to permanent damage.

The damage created by partial discharge activities is usually irreversible. This type of damage usually results in carbonized tracks that extend between the electrodes along the surface, leading in this way to a degradation of the insulation.

1.3 Methods of Fault Diagnosis for Power Transformer

1.3.1 Dissolved Gas Analysis

Dissolved gas analysis (DGA) is the study of dissolved gases in transformer oil. Insulating materials within transformers and electrical equipment break down to liberate gases within the unit. The distribution of these gases can be related to the type of electrical fault, and the rate of gas generation can indicate the severity of the fault. The identity of the gases being generated by a particular unit can be very useful information in any preventative maintenance program [21]. For this purpose, DGA has been a key tool for power transformer incipient fault diagnosis. It includes many successful approaches under three major categories: ratio methods, key gas

method, and artificial intelligence based methods. Ratio method is the most popular application used for a dissolved gas diagnosis. Table1.1 shows the ratio definition of ratio methods, it depends on the fix ratio of six gasses and four of them is used in Dorneenburg's ratio method as table1.2.

Table 1.1: Ratio definition of ratio methods

Ratio	CH_4/H_2	$C_2H_2/C_2/H_4$	C_2H_2/CH_4	C_2H_6/C_2H_6	C_2H_4/C_2H_6
Abbreviation	$R1$	$R2$	$R3$	$R4$	$R5$

Table 1.2: Dornenburg's ratio method

Fault	$R1$	$R2$	$R3$	$R4$
Thermal Decomposition	> 1.0	< 0.75	< 0.3	> 0.4
Corona(low intensity PD)	< 0.1	Not significant	< 0.3	> 0.4
Arcing(high intensity PD)	> 0.1 and < 1.0	> 0.75	> 0.3	< 0.4

According to the ratio method from the table, all the ratios were derived from experiment and have been recorded in code system. A fault condition is detected when a ratio code is matched as recording code. Using the relationship between the ratios of gasses with faults can predict a fault. The most widely used ratio methods is the IEC Standard 60599 which is depicted in Table 1.3 [21]. DGA has been widely used in monitoring of the power transformer due to it is convenience and reliability. Many DGA interpretative methods such as Key gas method [18], Dornerburg [18][20], Rogers [19] have been reported. The advantages of ratio method are quantitative and independent from transformer oil volume. However, ratio methods can produce incorrect interpretations. Therefore, ratio methods should be used in conjunction with other diagnostic methods such as the fuzzy diagnostic expert system[23].

Table 1.3: IEC code for DGA fault diagnosis

Range of gas ratio	$C_2H_2/C_2/H_4$	CH_4/H_2	C_2H_4/C_2H_6
< 0.1	0	1	0
$0.1 - 1$	1	0	0
1-3	1	2	1
> 3	2	2	2
Characteristic Fault	C_2H_2/C_2H_4	CH_4/H_2	C_2H_4/C_2H_6
Normal ageing	0	0	0
Thermal fault of low temperature$<$ 150degree	0	0	1
Thermal fault of low temperature between $150 - 300$degree	0	2	0
Thermal fault of medium temperature between $300 - 700$degree	0	2	1
Thermal fault of high temperature $>$ 700 degree	0	2	2
Partial discharge of low energy density	0	1	0
Discharges of low energy, Continuous sparking	1	0	1
Discharge of high energy, Arcing	1	0	2
Partial discharge of high energy density,Corona	1	1	0

1.3.2 Frequency Response Analysis

Winding deformation is the most common fault caused by mechanical or electrical failure in power transformers. Mechanical failure gives rise to the change of winding the structure, which occurs in transportation between the manufacturer and the service location. The short circuit is the main electrical fault in the power transformer, which results in the lightning strikes, so it can be modified by the impedance parameters of the windings, and resultant effect on the windings. Also, degradation of insulation can influence the winding structure. Frequency response analysis(FRA) widely employed into the winding deformation, which produce high efficiency measurement in detecting the winding deformation.

FRA is an ideal monitoring method for power transformer in the condition of transmission and distribution network, based on analysis AC impedance and any Resistor-Inductor-Capacitor (RLC) networks. Transformer modeling gives the characteristic parameter value of capacitance, resistance, self-inductance and mutual inductance. From this value the transfer function can be obtained, which is a generic term defined as a complex frequency response function.

Transfer function is the ratio between input and output. Hence, by selecting the notion in large power transformer models. Then calculating the voltage and current using fourier transform function to denote the ratio of them. All values of input and output depend on the values of characteristic parameters, since the variation of the winding structure corresponds to the changing of parameters. Frequency response analysis of electrical engineering is based on AC impedance or admittance, especially at relative high frequencies in the range of 100 kHz to 5 MHz. Potential factors caused by minor displacements in the geometric structure of large power transformer windings can be detected by FRA. In fact, FRA measurements can illustrate that changes in the dielectric parameters of the insulation system, which is caused by the temperature and moisture content of the insulating oil and cellulose paper[22].

1.3.3 Partial Discharge Analysis

As mentioned before, partial discharge(PD) is the main influence on transformer insulation aging or degradation. It can cause the insulation to age and fail and the insulation can eventually be damaged. Therefore, partial discharge is an early sign of transformer internal insulation degradation. According to the on-line monitoring the potential failure of transformer insulation can be detected and the degradation of insulation can be analysed. Monitoring of partial discharge is a vital function for improving the reliability of the transformer and their life cycle. The immediate response to partial discharge is to locate the discharge area quickly and accurately. Detection of partial discharge can be achieved by a variety of techniques: electrical methods, acoustic methods and ultra high frequency measurements. There are three types of analysis methods, i.e., time-resolved partial discharge analysis, intensity spectra based PD analysis, and phase resolved partial discharge analysis.

Electrical Method

The electrical method has been widely used for measuring transformer partial discharge. It mainly depends on the current sensor, which detects pulse current between ground and winding when partial discharge happens. The main advantage is higher sensitivity detection, and a strong ability to resist electromagnetic interference, while the disadvantage is that the test frequency range is low.

Ultra High Frequency Measurements

Partial discharge in the transformers can produce positive and negative charges. The steep current electromagnetic pulse generated can produce radiation. Ultra high frequency measurement refers to receiving ultra electromagnetic waves generated by partial discharge to detect partial discharge location. The range of frequency can be adjusted by using this method, and also it can prevent electromagnetic interference.

Acoustic Methods

Acoustic methods can detect the pressure fluctuations from PD. Several sensors are attached in the transformer vessel, and using digital technique is used

to detect the PD. The methods are used on-line and the spurious signals can be suppressed as much as possible. However, it cannot be calibrated and used as reference measurement.

1.4 Outline of the thesis

The first part of this thesis is ontology and its application to the diagnosis of power transformer failure. The second part investigates power transformer winding modeling and condition assessment using Frequency Response Analysis (FRA). The third part is using optimisation method to identify the parameters of a FRA model, for further improving the model accuracy of high frequency range. The thesis is structured as follow:

Chapter 2 introduces ontology based intelligence techniques and how to utilise it to detect power transformer faults.

Chapter 3 introduces partial discharge location in transformer windings by using multi-conductor transmission line model.

Chapter 4 reviews lumped parameter model of power transformer for FRA and comparison of results from the frequency response analysis with improved lumped model.

Chapter 5 proposes a model-based identification approach based on the basis of FRA measurements of power transformer parameters using optimisation method.

Chapter 6 concludes the thesis and summarises obtained results. Propesctive directions of further research are also discussed.

Chapter 2

Ontology and Power Transformer Diagnosis

2.1 Introduction to Ontologies and Web Ontology Language

Historically, ontologies arise out of the branch of philosophy known as metaphysics, which deals with the nature of reality of what exists. This basic branch is concerned with analysing various types or modes of existence, often with special attention to the relations between particulars and universals, between intrinsic and extrinsic properties, and between essence and existence. Traditional ontological target investigation, in particular, the world divided into the discovery of the "joint" of these basic categories or types, the object of natural decline [24].

In the second half of the 20th century, philosophers widely discussed possible approaches or methods to building an ontology, without establishing any very delicate ontology. Computer scientists, by contrast, build a few large and robust ontology, such as WordNet and Cyt, with relatively little debate how they build.

Since the mid - 1970s, researchers in the field of artificial intelligence (AI) that have discovered that knowledge is the key to building a powerful artificial intelligence system. Artificial intelligence researchers think that they can create a new ontology as the calculation model, make some kinds of automatic reasoning. In the

1980 s, the world of artificial intelligence community began to use the term "ontology" to refer to the modeling theory and the knowledge system of a component. Inspired from philosophical ontology, some researchers think that computing application ontology, as a philosophy [25].

In the early 1990 s, the widely quoted Web page and paper, the design principle of ontology for knowledge sharing," by Tom Gruber for deliberate ontology as the definition of computer science and technology term. Gruber introduces the term means a conceptualization of specification.

An ontology is a description (such as a formal specification of the program) and the concept of relationship, which can officially exist between an agent or representative of the community. This definition is commonly associated with the concept of ontology although this is a different from its use in the philosophical sense [27].

2.1.1 The Components of Ontology

Contemporary ontologies share many structural similarities, regardless of the language in which they expressed. As mentioned above, most ontologies describe individuals (instances), classes (concepts), attributes, and relations. Common components of ontologies include:

- Individuals: instances or objects (the basic or "ground level" objects)
- Classes: sets, collections, concepts, classes in programming, types of objects, or kinds of things
- Attributes: aspects, properties, features, characteristics, or parameters that objects (and classes) can have
- Relations: ways in which classes and individuals can be related to one another
- Function terms: complex structures formed from certain relations that can be used in place of an individual term in a statement
- Restrictions: formally stated descriptions of what must be true in order for some assertion to be accepted as input

- Rules: statements in the form of an if-then (antecedent-consequent) sentence that describe the logical inferences that can be drawn from an assertion in a particular form
- Axioms: assertions (including rules) in a logical form that together comprise the overall theory that the ontology describes in its domain of application. This definition differs from that of ”axioms” in generative grammar and formal logic. In those disciplines, axioms include only statements asserted as a priori knowledge. As used here, ”axioms” also include the theory derived from axiomatic statements
- Events: the changing of attributes or relations

2.1.2 OWL WEB Ontology Language

The OWL Web ontology language(OWL) is an international standard coding and exchange ontology and designed to support the semantic network. The concept of semantic web, information should be given specific meaning, so the machine can process more intelligently. Rather than only create a standard term is in extensible Markup Language (XML), the concept of semantics the site also allows the user to provide the formal definition of standard terms by them. The machine can use reasoning algorithm terms and conditions. Furthermore, if two different sets of terms are in turn defined using a third set of common terms, then it is possible to automatically perform (partial) translations between them. It envisioned that the Semantic Web will enable more intelligent search, electronic personal assistants, more efficient e-commerce, and coordination of heterogeneous embedded systems.

OWL is used as an ontology language for the Web. In 2004, it had become a World Wide Web Consortium (W3C) Recommendation. As such, it was designed to be compatible with the extensible Markup Language (XML) as well as other W3C standards. In particular, OWL extends the Resource Description Framework (RDF) and RDF Schema, which also endorsed by the W3C. Syntactically, an OWL ontology is a valid RDF document and as such also a well-formed XML document. Thus, OWL is available to process by XML and RDF tools.

Semantically, the OWL is based on description logic [26]. In general, can decide the description logic, is a logic family piece of first order predicate logic. These logical descriptions are based on classes and character, the set - theoretic semantics. Different description logics includes different subsets of logical operators.

Ontologies have been used to exchange information and knowledge representation in a variety of domains. The importance of ontologies has been widely accepted within the multi-agent community, in which they are employed, for example, for agent communication and knowledge sharing [29][30]. In order to successfully support these activities, an ontology should be rich enough in terms of knowledge representation and have a consistent interpretation.

2.1.3 Semantic Web

The Semantic Web is a clear vision of the future of Web information, the meaning of convenient machine automatic processing and integration of information available on the internet. The semantic Web will based on RDF and XML ability to define custom tag plans and flexible data representation. The first level above the RDF semantic Web ontology language to formally describe the meaning of the terminology used in the Web document. If the machine is expected to present useful reasoning tasks, these documents must go beyond the language of the basic semantic RDF schema. OWL use cases and requirements document to provide more details of the ontology, the incentive needs a Web ontology language six cases and develop design objectives, needs and goals of the OWL.

OWL is designed to meet the requirements of the Web ontology language. The OWL is a W3C recommendation part of the stack of the semantic web.

- XML provides a structured document of surface syntax, but has no semantic constraints on the significance of these files.
- XML Schema is a language, which is restricted of the structure of XML documents and also extends XML with datatypes.
- RDF is a data model object and the relationship between them, providing

a simple semantic data model, and these data models can be represented in XML syntax.

- RDF Schema is a vocabulary for describing properties and classes of RDF resources, define a semantics for generalization-hierarchies of such properties and classes.

- OWL added more information to describe attributes and classes: among them, the relations between classes, base, equality, the rich characteristics of the type attribute, and enumerated classes.

2.1.4 Ontology Languages

OWL provides three increasingly expressive sub-languages designed for use by specific communities of implementers and users as below:

OWL Lite supports user primarily needed a classification hierarchy and simple constraints. For example, although it supports cardinality constraints, it only allows a base value of 0 or 1. Should be simple to provide tools support OWL Lite is more expressive than its relatives, and OWL Lite for thesaurus provides a quick migration path and another classification. OWL Lite has a formal complexity which is lower than the OWL DL, see the section on Owl Lite part reference for more details.

OWL DL support users that want the biggest performance, while maintaining the computational completeness (all conclusion guarantee can calculate) and decidability, which means all computing need to be completed in a limited time. OWL DL includes all OWL language structures, but they can be used only in a certain limit (for example, a class may be a subclass of the class, class cannot be an instance of another class). OWL DL is so named because it conforms to the description logic, the research of this field has studied logic, form the basis for formal OWL.

2.1.5 *Protégé* Software Description

Protégé is a free, open source ontology editor and knowledge-base framework. The *Protégé* platform supports two main ways of modeling ontologies via

the $Protégé$-Frames and $Protégé$-OWL editors. $Protégé$ ontologies can be exported into a variety of formats including RDF, RDFS, OWL, and XML Schema. $Protégé$ is based on Java, is extensible, and provides a plug-and-play environment that makes it a flexible base for rapid prototyping and application development. Examples are a visual editor for OWL (called OWLViz), storage back-ends to Jena and Sesame, as well as an OWL-S plugin, which provides some specialized capabilities for editing OWL-S descriptions of Web services.

2.1.6 Graphviz

Graphviz is open source graph visualization software. Graph visualization uses abstract graphs and networks to represent structural information. It has already been applied onto the internet, bioinformatics, software engineering, database and web design, machine learning, and in visual interfaces for other technical areas.

The Graphviz layout scheme is described in a simple text language, and made useful chart formats, such as images and SVG web page; PDF or Postscript in other files, or displayed in the interactive graphical browsers. Graphviz has many useful features for concrete diagrams, such as options for colors, fonts, tabular node layouts, line styles, hyperlinks, and custom shapes.

2.2 Building a Model for Power Transformer Faults Based On Protege

During power system operation, maintenance and fault diagnosis decisions are often made by engineers by comparing the current state of the system with knowledge or experience gained from similar situations in the past.

An ontology describes concepts and relationships in a particular domain[31]. A transformer diagnosis ontology model is based on the concepts of transformer failure mode and analyses the relationship between each fault with reason. The key point in building such a model is to identify the relationships between relevant part then set them as classes, individuals and properties. There are mainly

three power transformer failure models, electrical failure, mechanical faults, partial discharge faults. Each fault can be caused by different reasons, and interactions between them. However, it may be difficult for an expert to express the reasoning process involved, for implementation in a computer system. Therefore, it is useful to provide a structured knowledge representation mechanism which can be used to encode the knowledge of domain experts for use in automated reasoning systems. $Protégé$ is a software for this purpose. It has following steps:

- Creating a new OWL project
- Creating a class
- Creating some subclasses
- Creating some properties
- Creating some individual

The basic structure of the proposed fault diagnosis system has three main parts: transformer failure models, diagnosis method, and fault phenomenon.

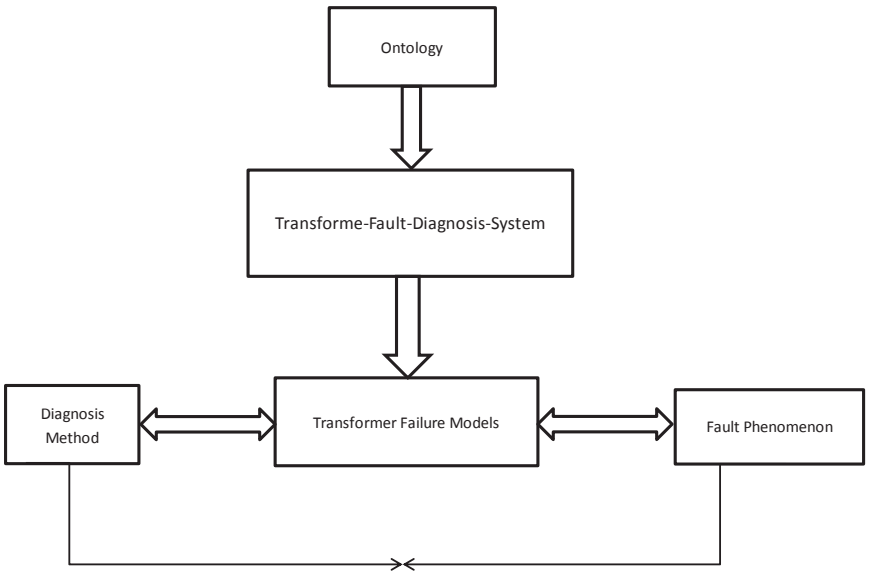

Figure 2.1: Structure of transformer fault diagnosis system

2.2.1 Named Classes

The main structure of an OWL ontology are classes, to build a transformer failure mode will set it as classes. In $Protégé$, editing of classes is carried out using the 'Classes Tab' shown in Fig. 2.2. The empty ontology contains one class called Thing. As mentioned previously, OWL classes are interpreted as sets of individuals (or sets of objects). The class Thing is the class that represents the set containing all individuals. Because of this all classes are subclasses of Thing.

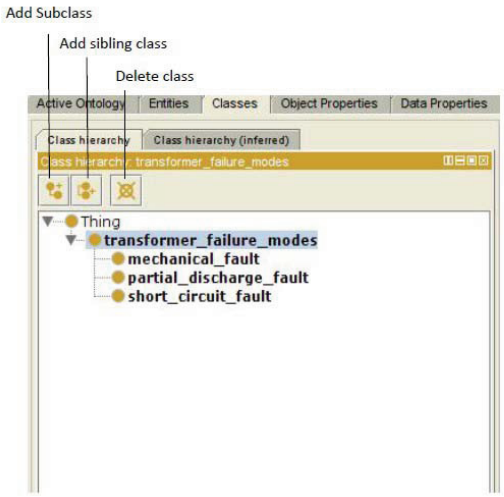

Figure 2.2: The Classes Tab

2.2.2 Creating Subclasses

Having added the classes "electrical failure mode", "mechanical fault" and "partial discharge fault" to the ontology model. It is said these classes are classes of the transformer failure mode in Fig. 2.3.

In the same way, one can increase the structure of the classes by adding more subclasses as Fig. 2.4.

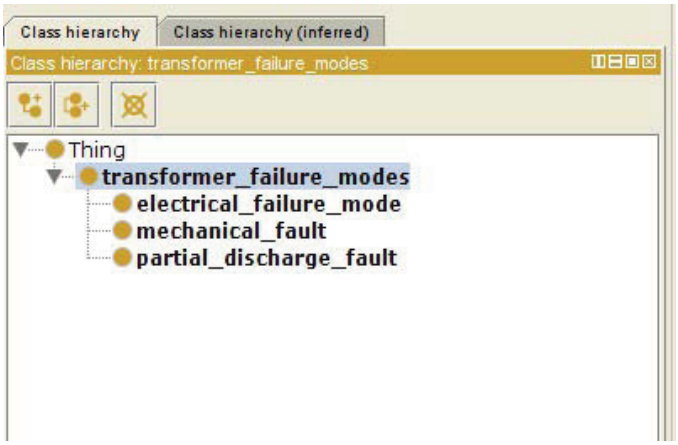

Figure 2.3: Subclass of transformer failure model

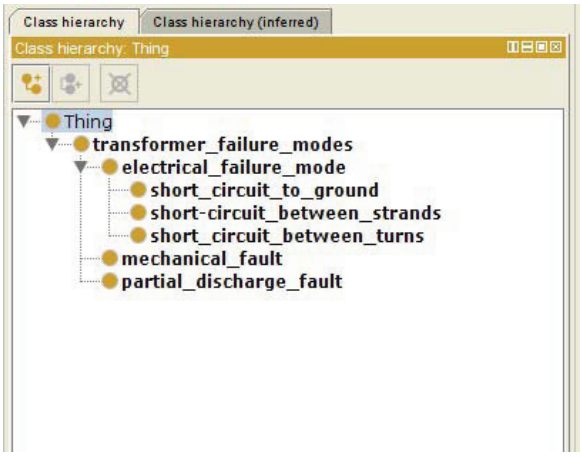

Figure 2.4: Subclass of electrical failure model

2.2.3 OWL Properties

There are two main types of properties, Object properties and Datatype properties.

Object Properties are relationships between two individuals. Properties may be created using the 'Object Properties' tab. Fig. 2.5 shows the buttons located in the top left hand corner of the 'Object Properties' tab that are used for creating

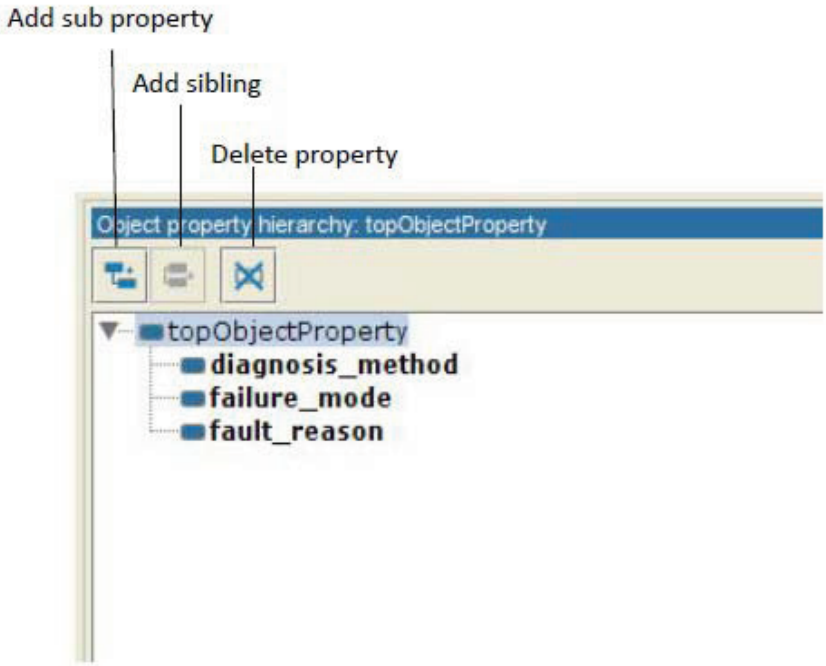

Figure 2.5: Property creation buttons

Inverse Properties Each object property may have a corresponding inverse property. If some property links individual 'a' to individual 'b' then its inverse property will link individual 'b' to individual 'a'. For example, in power transformer faults of gassing and overheating, both of them can interact with

each other, like temperature over $700°C$ degree will generate gassing in transformer, Fig. 2.6 shows the property 'hasoverheating' and its inverse property 'hasgassing', therefore, if overheating can cause gassing, then because of the inverse property it can infer that gassing is caused by overheating.

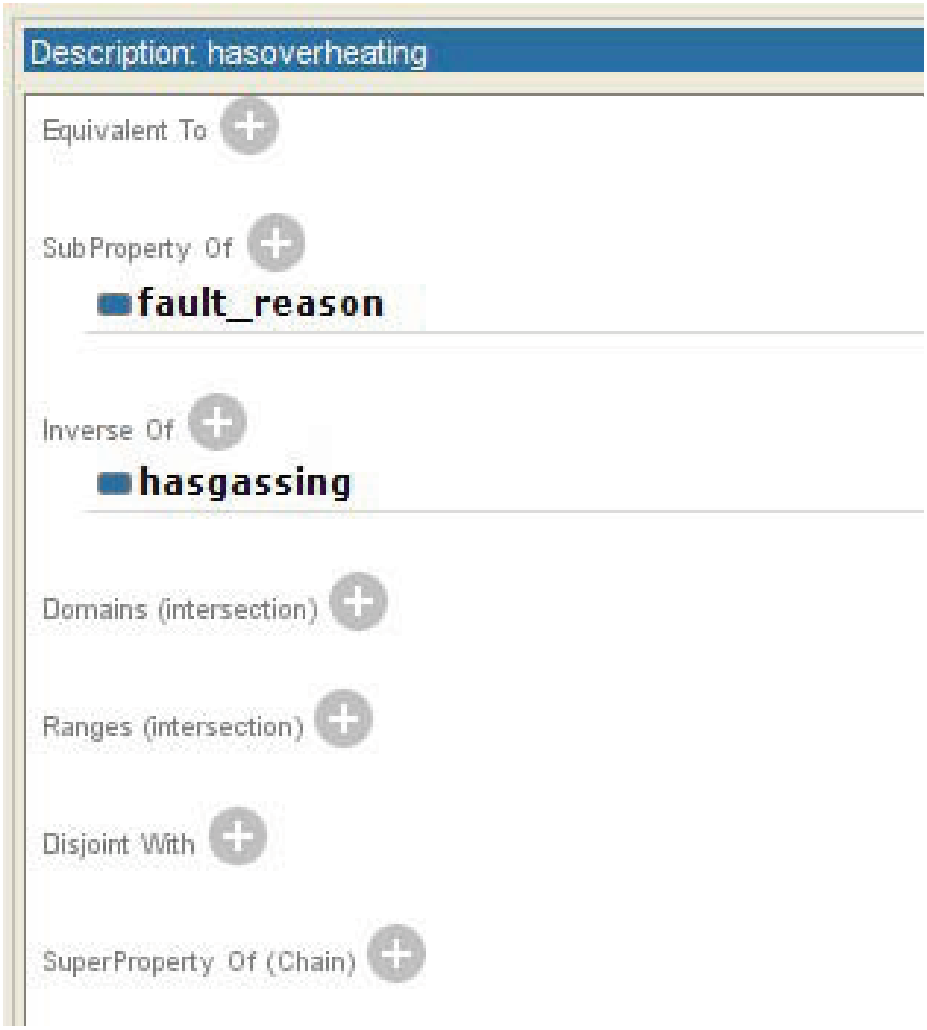

Figure 2.6: The inverse property

Datatype Properties Datatype properties link an individual to an XML Schema Datatype value or an RDF literal. In other words, they describe relationships between an individual and data value. Datatype properties can be created using the Datatype Properties view in either the Entities or Datatype Properties.

As mentioned before, local overheating will generate the gassing in power transformers. Considering the value of temperature in different situations is useful to denote the type of gases generated. For example, temperature over 700 degree will generate $CH4$, $CH2$, $C2H4$, $C2H2$,$C2H6$, on the other hands, the ratio of gassing is relative to the value of temperature. Use datatype properties to describe local overheating in the power transformer, create several datatype property include $CH4/CH2$, $C2H4/C2H6$, $C2H2/C2H4$,$C2H6/CH4$, which will be used to state the gassing. Firstly adding $CH4/CH2$, $C2H4/C2H6$, $C2H2/C2H4$,$C2H6/CH4$ as data property, then set up the range of them as decimal in Fig. 2.7. Secondly, add temperature over 700 degrees in Class section, select class Description view' of temperature over 700 degree type values of each ratio of gasses as Fig. 2.8.

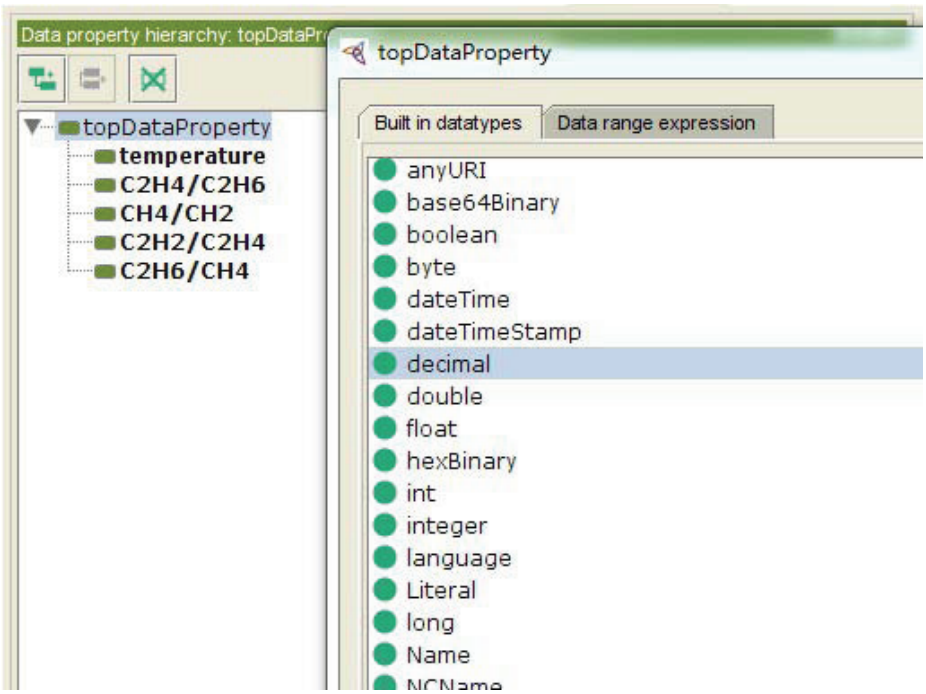

Figure 2.7: Create datatype property using $protégé$

Data type properties can use with individual specific data type or untyped. Data type properties can also be used to limit the individual members of a given data type. Based on the XML schema data types is specified vocabulary

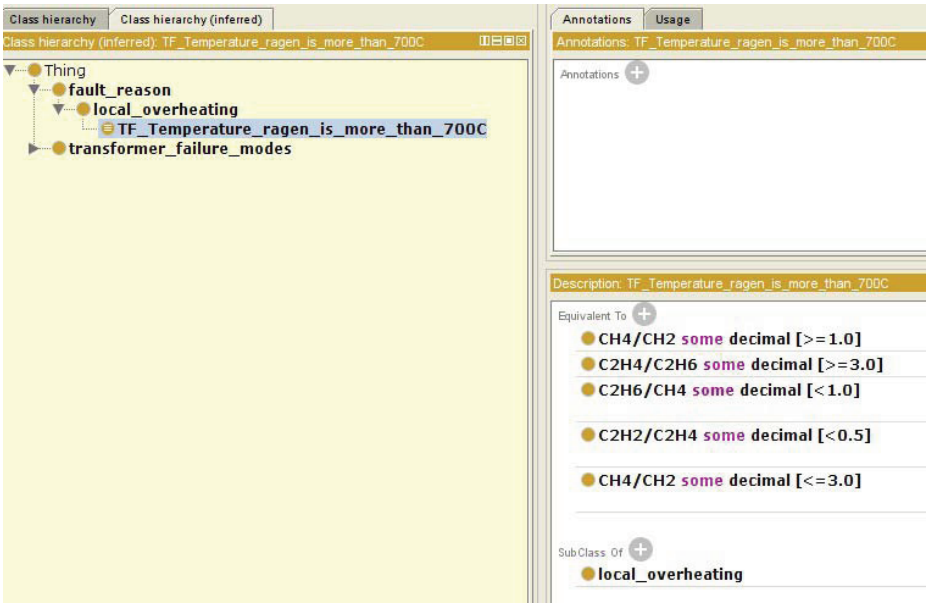

Figure 2.8: Using datatype restrictions to define ranges for ratio of gasses

and including an integer, floats, text, decimal, etc.

DL Query The DL Query tab provides a powerful and easy-to-use feature for searching a classified ontology. It is a standard $Protégé 4.3$ plugin, available both as a tab and also as a view widget that can be positioned into any other tab. The query language (class expression) supported by the plugin is based on the Manchester OWL syntax, a user-friendly syntax for OWL DL that is fundamentally based on collecting all information about a particular class, property, or individual into a single construct, called a frame. DL query TAB provides a powerful searching classification ontology and easy to use features. It is a standard $Protégé$ four plug-ins, can be used as a tab, and can also locate to any other TAB. Support query language (expression) plug-in is based on the special OWL syntax, a user-friendly grammar OWL DL, is fundamentally based on collecting all information about a particular class, property, or personal as a structure, called a frame.

Individual Query Examples The last part already describes using data type to illustrate the overheating problem, like this:

- class:
  - overheating
  - temperature is over $700°C$
- data properties:
  - $CH4/CH2$
  - $C2H4/C2H6$
  - $C2H6/CH4$
  - $C2H2/C2H4$

And suppose also that gassing in overheating in our ontology. To find when $CH4/CH2$ have value as 2.5 and $C2H2/C2H4$ has value as 0.14 and enter the following query:

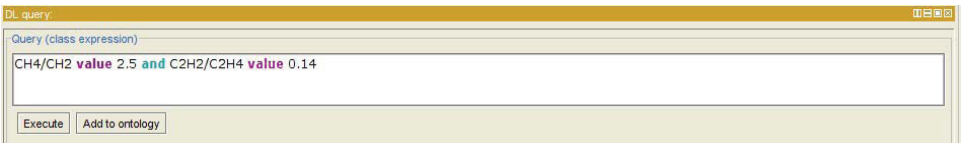

Figure 2.9: Class expression of query

Any results found will then be displayed in the query results as shown below: Fig. 2.10.

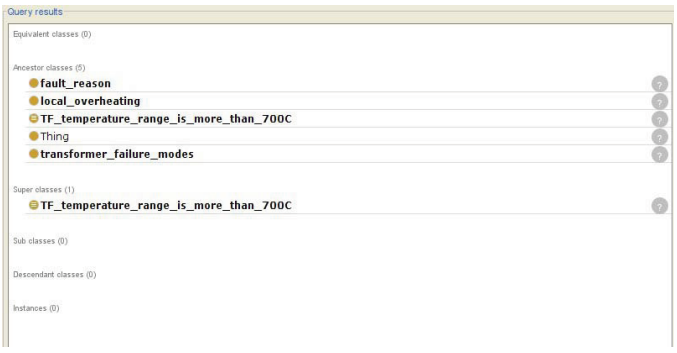

Figure 2.10: Results shown in DLquery

Here is another example of class queries that can be performed on the ontology of photography (work in progress). Questions about temperatures over $700°C$ is shown in Fig. 2.11, engineers can consider the results to denote the typical gasses easily.

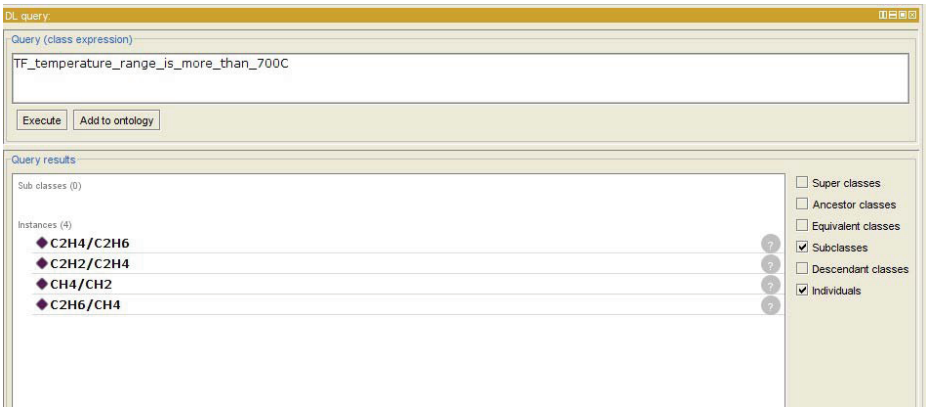

Figure 2.11: Individual of temperature over $700°C$

OWLviz OWLViz is designed to be used by the $Protégé$-OWL editor. It makes an OWL ontology in the class hierarchy incrementally viewing and navigation, to assert that the class hierarchy of comparison and infer the class hierarchy. OWLViz integrates $Protégé$- OWL editor, uses the same color scheme. Such basic can distinguish and define the class, class hierarchy changes could see clearly, and inconsistent concepts are highlighted in red. OWLViz has facilities to save assertions and conclude that the class hierarchy views specific graphics formats include PNG, JPEG and SVG.

2.3 Simulation Results and Analysis

2.3.1 Proposed Ontology Model for Electrical Failure

In this section, $Protégé$ is used to represent electrical failure models, including short-circuit between turns (SCBT), short-circuit between strands (SCBT),

short-circuit to ground (SCTG), floating potential (FP), short-circuited core laminations (SCCL), multiple core grounding (MCG), and ungrounded core (UC). Subclasses of electrical failures models are shown by OntoGraf in Fig. 2.12. The structure of the designer ontology model can be displayed by OnLVIZ with Graphviz in $Protégé4.3$, shown in the Fig. 2.13.

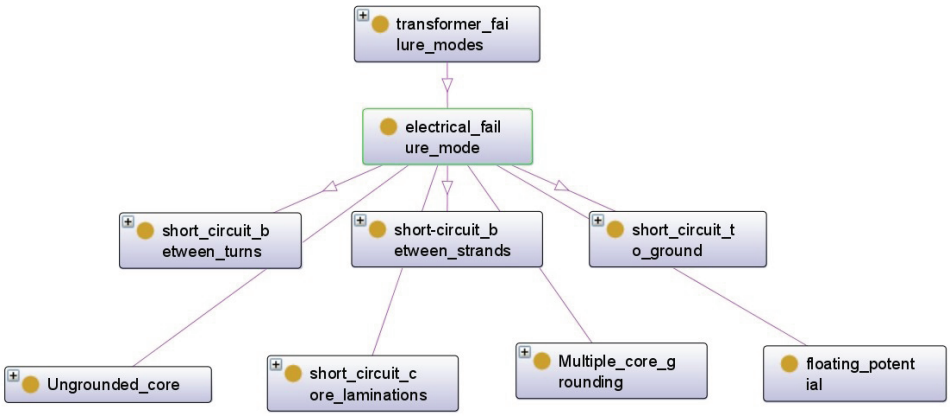

Figure 2.12: Subclasses of electrical failures models

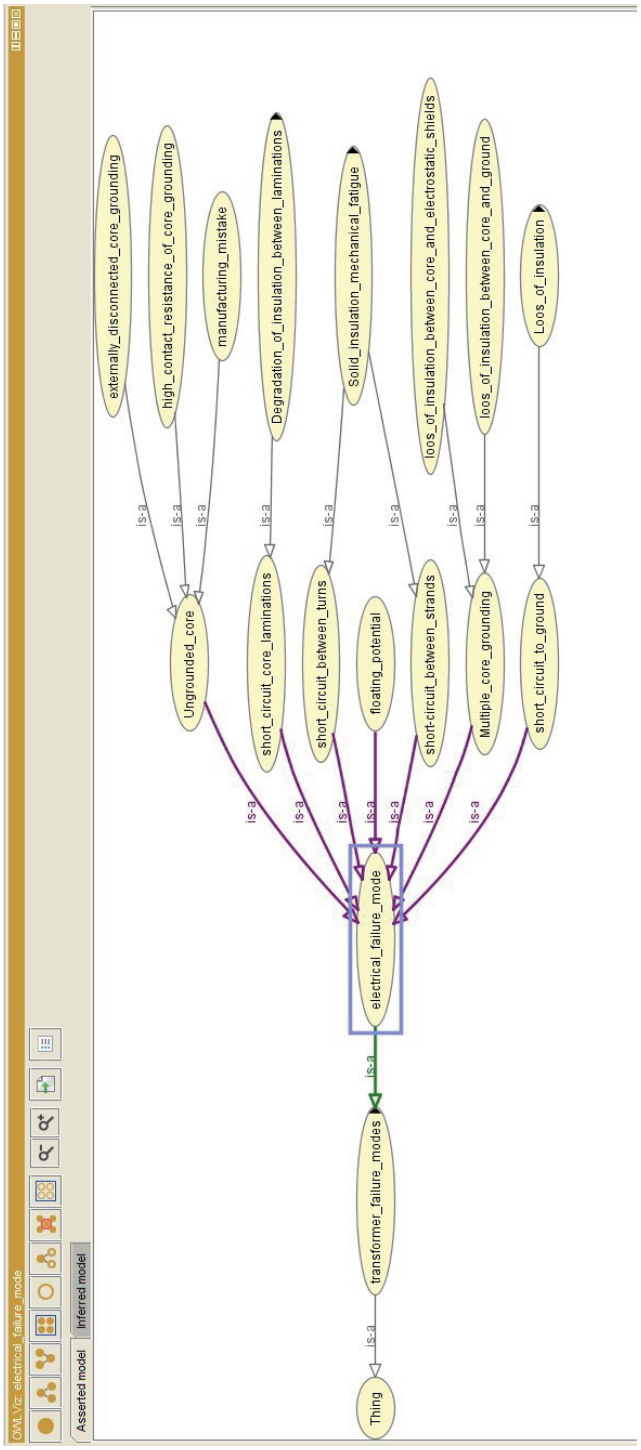

Figure 2.13: OWLviz graph

OntoGraf shows relationships and node types, which can be filtered to help the designer to creat the view their desire. Fig. 2.14 to Fig. 2.18 show the each mechanism of electrical failure models. Referring to all graphs, short-circuit between turns is complex and can be caused by different reasons. In order to avoid short-circuit to turn, high temperature, gassing, load component in exciting current, change in a number of turns, and reduction of winding resistance need to be monitored.

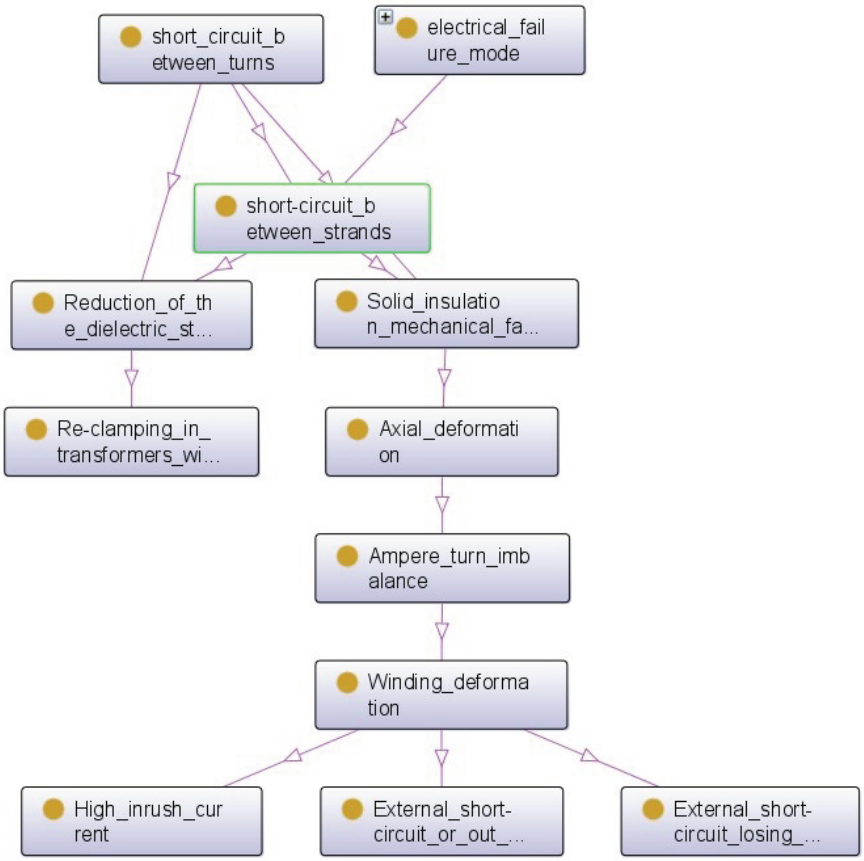

Figure 2.14: Short circuit between strands

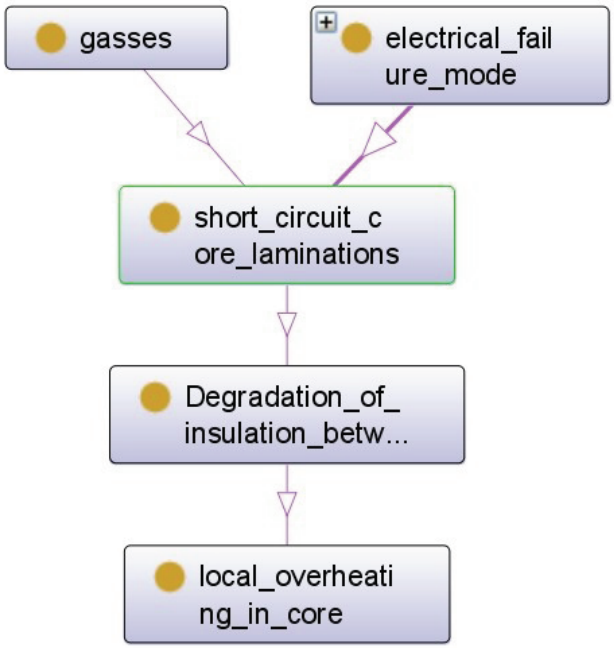

Figure 2.15: Short circuit core laminations

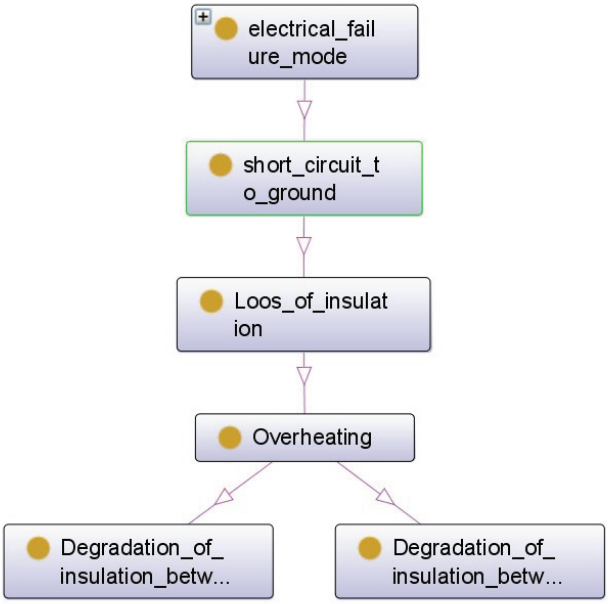

Figure 2.16: Short circuit to ground

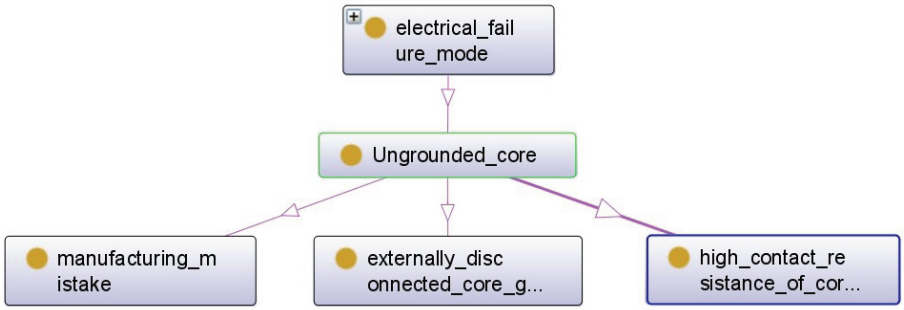

Figure 2.17: Ungrounded core

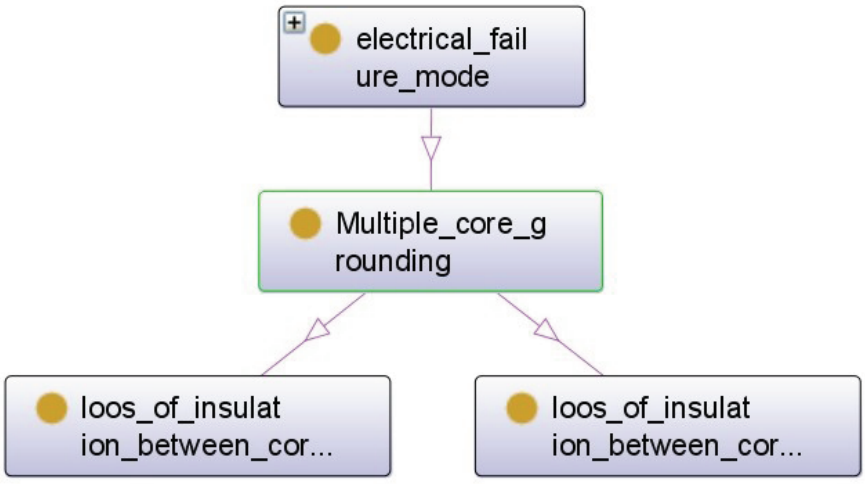

Figure 2.18: Multiple core grounding

2.3.2 Proposed Ontology Model for Protection Trip

Fig. 2.19 presents two protect trips, buchholz protection trips and normal protection trip. Buchholz have two functions. Firstly, it is a sudden pressure trip, which can be replaced by a rapid pressure rise relay of a transformer. This provides protection for major faults, such as expanding gas, and major oil leaks. Secondly, it can detect gas accumulation by an alarm. This provides early warning alarms for core faults, internal faults, and faulty joints. Those faults also can be detected by electronic monitoring equipment such as partial discharge or online dissolved gas monitoring, but is much more expensive than a Buchholz. Fig. 2.20 presents that structure of gassing with buchholz protection trips.

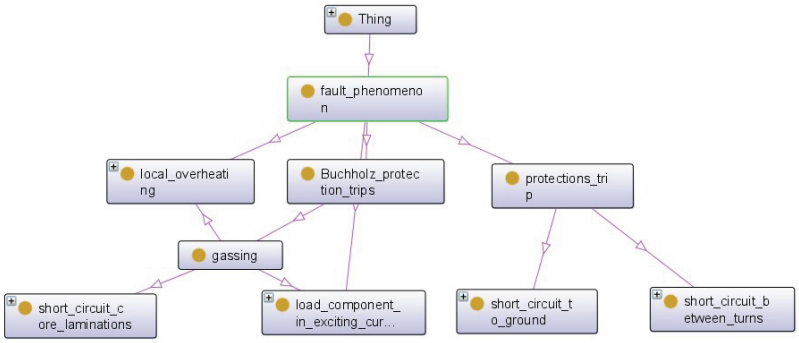

Figure 2.19: Structure of protection trip and buchholz protection trips

2.3.3 Proposed Ontology Application of DGA Methods

As above discussed, the high ratio value of gasses will cause a number of failure models, and also some failure models will produce an amount of gasses such as short-circuit between turns. On-line detection of the value of gasses is very important in power transformer diagnostic. Initial Roger's Ratios is used to describe originally developed four ratios of values of main

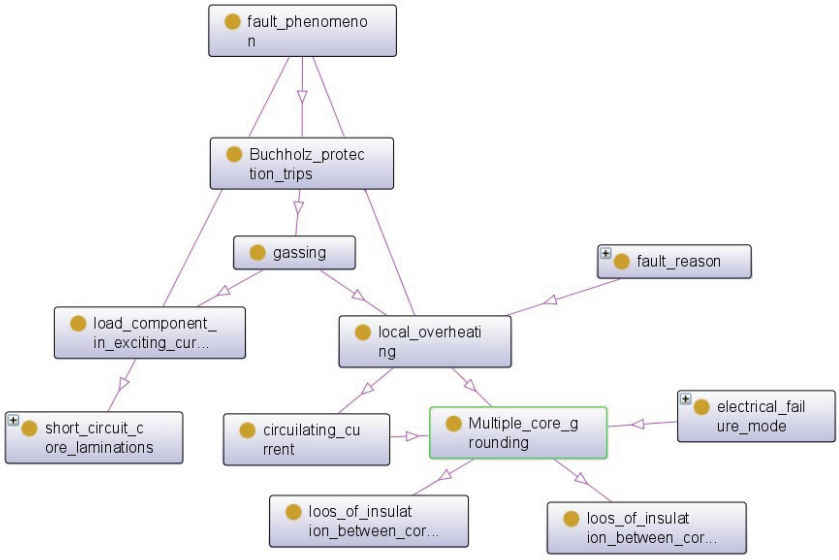

Figure 2.20: Structure of gassing with buchholz protection trips

gasses in power transformers, include CH4/H2, C2H4/C2H6, C2H6/CH4 and C2H2/C2H4[33][34].

Table 2.1: Initial Roger's Ratios

CH_4/H_2	≤ 0.1	5
	$> 0.1 > 1$	0
	$\geq 1 < 3$	1
	≥ 3	2
C_2H_6/CH_4	< 1	0
	≥ 1	0
C_2H_4/C_2H_6	< 1	0
	$\geq 1 < 3$	1
	≥ 3	2
$C_2H_2/C_2/H_4$	< 0.5	0
	$\geq 0.5 < 3$	1
	≥ 3	2

Table 2.2: Initial Roger's Ratios

CH_4/H_2	C_2H_6/C_2H_4	C_2H_4/C_2H_6	C_2H_2/C_2H_4	Diagnosis
0	0	0	0	Normal
5	0	0	0	Partial discharge
$1/2$	0	0	0	slight overheating-below $150°C$
$1/2$	1	0	0	slight overheating- $150°C$ to $200°C$
0	1	0	0	slight overheating- $200°C$ to $300°C$
0	0	1	0	slight overheating- General conductor overheating
1	0	2	0	core and tank circulating currents overheated joints
0	0	0	1	Flashover without power follow through
0	0	$1/2$	$1/2$	Arc with power follow through
0	0	2	2	Continuous sparking to floating potential
5	0	0	$1/2$	Partial discharge with tracking

Table 2.1and Table 2.2 present the Roger's fault diagnosis. *Protégé*4.3 based on the Roger's fault diagnosis table to build an ontology models for failures:

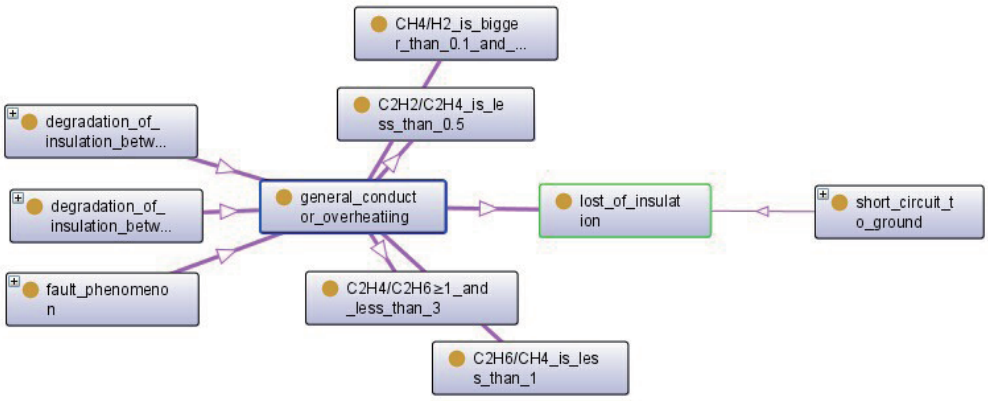

Figure 2.21: A structure of each class of general conduction overheating

Fig. 2.21 starts from a degradation of insulation between windings and core, and degradation of insulation between leads and ground, point to general conductor overheating, then produces the gassing, causes loss of insulation, terminates at short circuit to ground. Fig. 2.22 starts from buchholz protection trips, point to gassing, then find out local overheating and load component in exciting circulating current, terminates at short circuit core lamination and multiple core grounding. Fig. 2.23 shows an ontology model of general conductor overheating.

An ontology model can help to denote the reason for the problem and find out the relationship between each part in power transformers. Ontology models can provide more information including numerous classes and a large relationship network in the power transformer diagnosis system, it can more quickly and more exactly help engineers to find out the reasons and correction solutions.

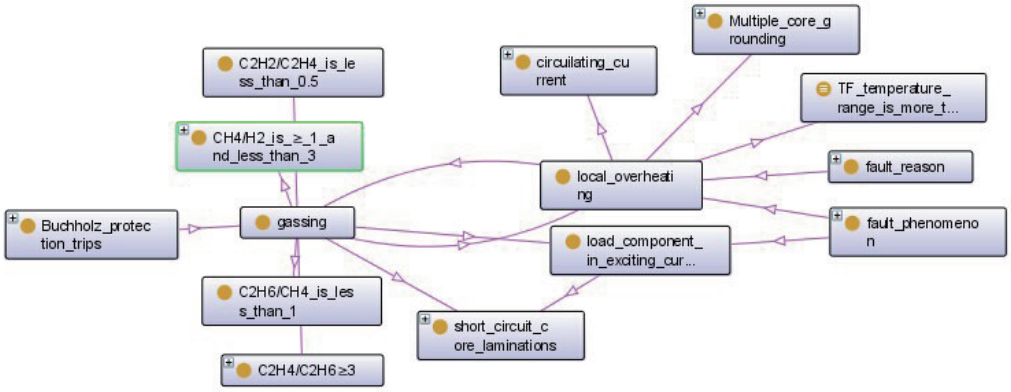

Figure 2.22: Ontology model of gassing fault

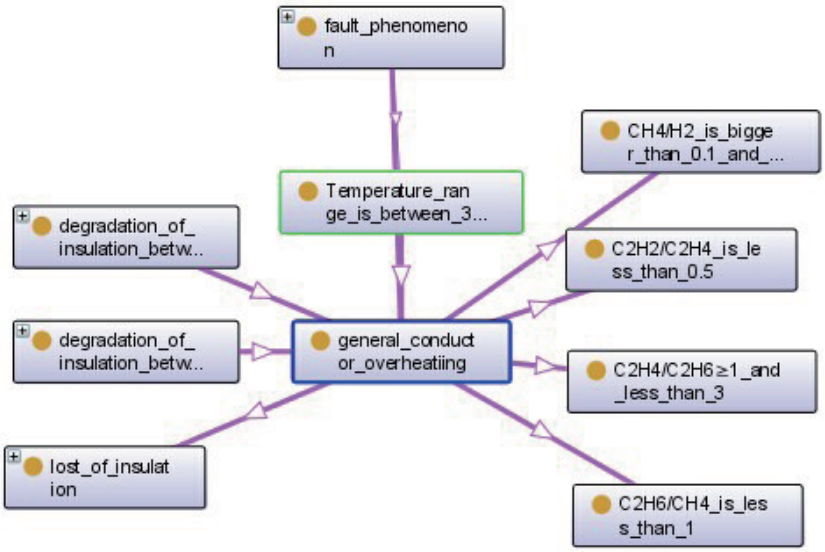

Figure 2.23: Screen shot from OntoGraf

2.4 Summary

This chapter provides a brief introduction to the ontology concept and how to build up a model by using the ontology. Ontology models are based on the specification concept of knowledge and are used to analyse various concepts and relationship networks. $Protégé 4.3$ is the software used to build an ontology model for transformer fault diagnosis. An electrical failure model was built by $Protégé 4.3$. The developed model was integrated with dissolved gas analysis.

Chapter 3

Partial Discharge Location in Transformer Windings Using Multi-Conductor Transmission Line Model

3.1 Introduction

Partial discharge (PD) is a common fault in power transformers. It causes gradual degradation of power transformer insulation which may finally lead to a full breakdown. In order to avoid serious damage, it is better to quickly for locate partial discharges. Otherwise they will cause serious consequences. There are several methods that have been used in PD measurement, for example electrical method, ultra high frequency measurements, and acoustic methods. This chapter will mainly illustrate electrical method. Electrical PD measurement can be divided into narrowband and wideband [43]. Engineers consider the information from PD waveforms for the diagnosis of PD location in the transformer. Since the frequency range of large power transformers reaches up to MHz, the requirements of the PD detection system can satisfy

high frequency range. VHF systems are widely used and it can reach some MHz range, hence it has become possible to record single PD pulses with a high accuracy [44][45].

In practise, the most difficult aspect of the partial discharge method is to locate PD source. Once PD source has been located, maintenance cost and damage can be reduced. PD pulses that originate from a point inside the transformer are attenuated and distorted on their way to the detection point under the influence of winding transfer function. PD location will be more difficult to detect when the PD pulse is mixed with a variety of measurement noise and external disturbance. Therefore, the recorded signals must be preprocessed for noise suppression before it can be used for PD location.

In this chapter, multi-conductor transmission line model (MTLM) is introduced and used for the simulation of partial discharge. MTLM is one model for transformer winding [36]. In MTLM, each turn of the winding is modeled as a transmission line. The frequency range of MTLM is higher than the other models and usually reaches to several MHz. Hence, it is suitable for PD study. In practice, MTLM has been used for transformer modeling and its transfer functions can be used for finding the location of PD [46][47]. During measurement, extra attention has to be paid for selecting sampling frequency, vertical resolution and noise filtering. MTLM computations for large power transformers are too complex and time consuming hence its application in the industry becomes limited.

3.2 The Mathematical Construction Model

The multi-conductor transmission lines (MTL) model views every disc of a transformer winding as a transmission line and these lines are parallel with each other and the ground. Fig. 3.1 shows the connection of the transmission lines of the MTL model.

The analysis of signal propagation is based upon the Telegrapher's equa-

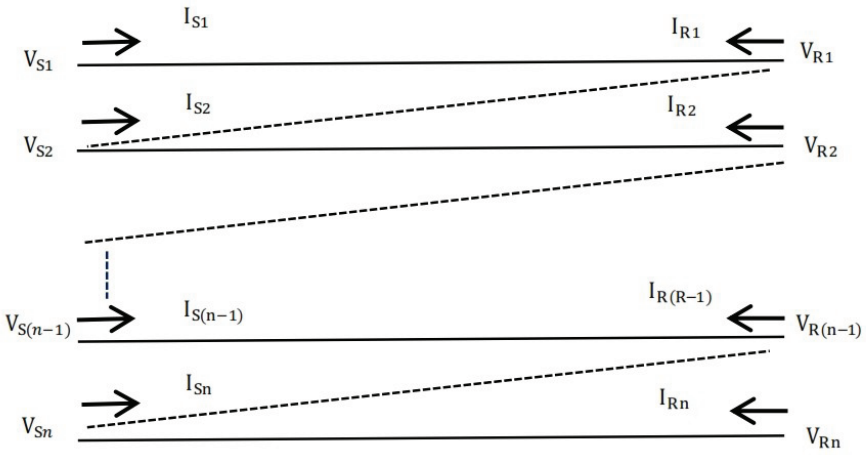

Figure 3.1: The connection of the transmission lines of the MTL model

tions for lossy transmission lines, which are expressed using the notations as follows 3.2.1[38]

$$\begin{cases} \dfrac{d\mathbf{U}}{dx} = -(sL+R)I = -ZI \\ \dfrac{d\mathbf{I}}{dx} = -QU + Y_s U \end{cases} \tag{3.2.1}$$

where U,I are the voltage and current vectors, L,R,C and G are the 'unit-length' inductance, resistance, capacitance and conductance $N \times N$ matrices, where N is the number of turns in a winding.

where

$$\begin{cases} Z_1 = & L_1 s + r_1 \\ Y_1 = & (C_1 + C_{d12})s + (G_1 + G_{d12}) \\ Y_{s1} = & K_1 s + g_1 \\ Q_{12} = & C_{d12} s + G_{d12} \end{cases} \tag{3.2.2}$$

$$\mathbf{Z} = \begin{bmatrix} Z_1 & sM_{12} & \dots & sM_{1n} \\ sM_{21} & Z_2 & \vdots & \dots \\ \vdots & \vdots & \ddots & sM_{(n-1)n} \\ sM_{n1} & \vdots & sM_{n(n-1)} & Z_n \end{bmatrix} \tag{3.2.3}$$

$$\mathbf{Q} = \begin{bmatrix} Y_1 & -Q_{12} & \dots & 0 \\ -Q21 & Y_2 & \ddots \vdots & \\ \vdots & \ddots & \ddots - Q_{(n-1)n} & \\ 0 & \dots - Q_{n(n-1)} & Y_n & \end{bmatrix} \tag{3.2.4}$$

$$\mathbf{Ys} = \begin{bmatrix} a^2 Y_{s1} & 0 & \dots & 0 \\ 0 & a^2 Y_{s2} & \dots & 0 \\ \vdots & \ddots & \ddots & \vdots \\ 0 & \ddots & sM_{n(n-1)} & a_Y^2 sn \end{bmatrix} \tag{3.2.5}$$

The equivalent circuit of a transform winding containing n disc is given in Fig. 3.2, where the following parameters per unit conductor length are used:

Equations3.2.1 and 3.2.2 yield the following equation:

$$\begin{cases} \dfrac{d\mathbf{U}_{(\mathbf{s},\mathbf{x})}}{dx} = -(sL + R)I = -ZI \\ \dfrac{d\mathbf{I}_{(\mathbf{s},\mathbf{x})}}{dx} = -QU + Y_s U = -YU \end{cases} \tag{3.2.6}$$

$$\frac{d}{dx} \begin{pmatrix} \mathbf{U}(s,x) \\ \mathbf{I}(s,x) \end{pmatrix} = A \begin{pmatrix} \mathbf{U}(s,x) \\ \mathbf{I}(s,x) \end{pmatrix} \tag{3.2.7}$$

where

$$\mathbf{A} = \begin{bmatrix} 0 & -Z \\ -Y & 0 \end{bmatrix} \tag{3.2.8}$$

with **0** the $n \times n$ zero matrix

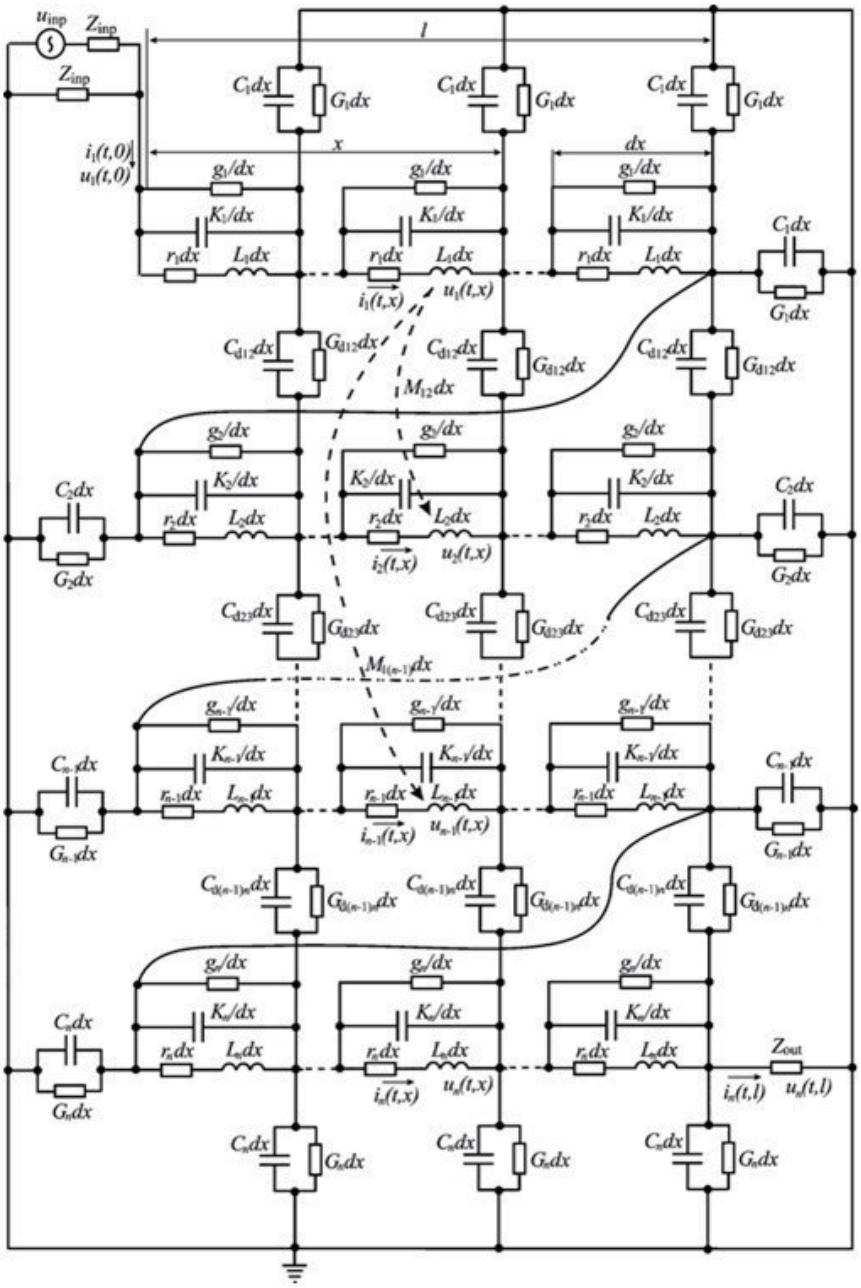

Figure 3.2: The equivalent circuit of a disc-type transformer winding[36]

The next task is to solve 3.2.7 and incorporate the boundary conditions. Let

$$\mathbf{X} = \begin{bmatrix} U \\ I \end{bmatrix} \tag{3.2.9}$$

then equation 3.2.7 becomes

$$\frac{d\mathbf{X}}{dx} = \mathbf{A}\mathbf{X} \tag{3.2.10}$$

The solution of matrix equation 3.2.7 for the voltages and currents at the ends of transformer winding, when $x = 0$ and $x = l$, is obtained in the form below:

$$\begin{bmatrix} \mathbf{U}(s,l) \\ \mathbf{I}(s,l) \end{bmatrix} = \phi(l) \begin{bmatrix} \mathbf{U}(s,0) \\ \mathbf{I}(s,0) \end{bmatrix} = \begin{bmatrix} \phi_{11}(l) & \phi_{12}(l) \\ \phi_{11}(l) & \phi_{22}(l) \end{bmatrix} \begin{bmatrix} \mathbf{U}(s,0) \\ \mathbf{I}(s,0) \end{bmatrix} \tag{3.2.11}$$

Transfer function for FRA of the MTL model is calculated as the ratio of Un(s,l)and U1(s,0):

$$H(s) = \frac{Un(s,l)}{U1(s,0)} \tag{3.2.12}$$

Equation 3.2.11 is rearranged in the form as below:

$$\begin{bmatrix} \mathbf{I}(s,0) \\ \mathbf{I}(s,l) \end{bmatrix} = \begin{bmatrix} \Upsilon_{11}(l) & \Upsilon 12(l) \\ \Upsilon_{11}(l) & \Upsilon 22(l) \end{bmatrix} \begin{bmatrix} \mathbf{U}(s,0) \\ \mathbf{U}(s,l) \end{bmatrix} \tag{3.2.13}$$

where

$$\begin{aligned} \Upsilon_{11}(l) &= -\Phi_{l2}(l)^{-1}\Phi_{11}(l) \\ \Upsilon_{12}(l) &= \Phi_{l2}(l)^{-1} \\ \Upsilon_{21}(l) &= \Phi_{21}(l) - \Phi_{22}(l)\Phi_{l2}(l)^{-1}\Phi_{11}(l) \\ \Upsilon_{22}(l) &= \Phi_{22}(l)\Phi_{l2}(l)^{-1} \end{aligned} \tag{3.2.14}$$

$$\begin{bmatrix} \mathbf{I}_1(s,0) \\ \mathbf{I}_2(s,0) \\ \vdots \\ \mathbf{I}_n(s,0) \\ \mathbf{I}_1(s,0) \\ \vdots \\ \mathbf{I}_n(s,0) \\ \mathbf{I}_n(s,0) \end{bmatrix} = \begin{bmatrix} \boldsymbol{\Upsilon}(l) \end{bmatrix} \begin{bmatrix} \mathbf{U}_1(s,0) \\ \mathbf{U}_2(s,0) \\ \vdots \\ \mathbf{U}_n(s,0) \\ \mathbf{U}_1(s,0) \\ \vdots \\ \mathbf{U}_n(s,0) \\ \mathbf{U}_n(s,0) \end{bmatrix} \tag{3.2.15}$$

where Υ is a $(n+1) \times (n+1)$ matrix. Finally, by inverting matrix $\Upsilon(l)$ can be rewritten as follows:

$$\begin{bmatrix} \mathbf{U}_1(s,0) \\ \mathbf{U}_2(s,0) \\ \vdots \\ \mathbf{U}_n(s,0) \\ \mathbf{U}_n(s,0) \end{bmatrix} = \begin{bmatrix} \boldsymbol{\Omega}(l) \end{bmatrix} \begin{bmatrix} \mathbf{I}_1(s,0) \\ \mathbf{I}_2(s,0) \\ \vdots \\ \mathbf{U}_n(s,0) \\ \mathbf{U}_n(s,0) \end{bmatrix} \tag{3.2.16}$$

where $\Omega(l) = [\Upsilon(l)]^{-1}$ is of $(n+1) \times (n+1)$ order.

3.3 Partial Discharge Location Method

The following boundary conditions can be seen in Fig. 3.1:

$$\begin{aligned} V_R(i) &= V_S(i+1) \\ I_R(i) &= -I_S(i+1) \end{aligned} \tag{3.3.1}$$

where $V_s(i)$ and $I_s(i+1)$ are sending end voltage and current of ith transmission line and $V_R(i)$ and $I_R(i)$ are its receiving end voltage and current.

In order to use MTLM for PD location, its equation must be modified briefly as follows. If it is supposed that a PD pulse has occurred in kth turn of the winding in Fig. 3.1, equation 3.3.1 will be modified for $i = k-1$ as:

$$I_R(k-1) + I_s(k) = I_{PD} \tag{3.3.2}$$

where I_{PD} is the PD pulse current. Applying the new boundary conditions of equation 3.3.1 and 3.3.2 and performing some simplifications and a matrix inversion, the voltages of transmission lines can be expressed in terms of currents as:

$$\begin{bmatrix} \mathrm{V}_s(1) \\ \vdots \\ V_s(k) \\ \vdots \\ V_s(n) \\ V_R(n) \end{bmatrix}_{(n+1).1} = [T]_{(n+1)(n+1)} \begin{bmatrix} I_s(1) \\ 0 \\ \vdots \\ I_{PD} \\ 0 \\ \vdots \\ I_R(n) \end{bmatrix}_{(n+1).1} \tag{3.3.3}$$

Transformer terminal conditions at the line-end and neutral end of the winding can be written as follow:

$$\begin{aligned} \mathrm{V_s}(1) &= -(Z + \tfrac{1}{j\omega C_B}) I_s(1) \\ V_R(n) &= -Z^{'} I_R(n) \end{aligned} \tag{3.3.4}$$

where Capacitance C_B as a sensor connected to the line-end which is to pick up PD pulse. Substituting the above terminal conditions in 3.3.3, the transfer function from PD source to the line-end(TFL) and also the transfer function from PD source to the neutral-end (TFN) are obtained as[40][39]

$$TF_L = \frac{Is(l)}{IPD} = \frac{\Omega_{(1,k)}(Z' + \Omega_{(n+1,n+1)}) - \Omega_{(n+1,k)}\Omega_{(1,n+1)}}{\Omega_{(1,n+1)}\Omega_{(n+1,1)} - (\Omega_{(1,1)} + Z + \frac{1}{jwC_B})(Z' + \Omega_{(n+1,n+1)})} \tag{3.3.5}$$

$$TF_N = \frac{IR(n)}{IPD} = \frac{-\Omega_{(n+1,1)}TF_L - \Omega_{(n+1,k)}}{Z' + \Omega_{(n+1,n+1)}} \tag{3.3.6}$$

The above equations show that only the frequency positions of zeros of transfer functions are related to the location of PD and the positions of poles are at fixed frequencies. In the proposed method in this paper, TFL and TFN are calculated from all possible PD locations to the line-end and neutral-end using

the above equation. All the simulation were achieved in the Matlab, includes calculating the components of matrix Ω from the model parameters and the terminal conditions of the transformer. Since $I_S(1)$ and $I_R(n)$ are in access from PD measurement at line-end and neutral-end, I_{PD} can be calculated by equation 3.3.5 and equation 3.3.6. Theoretically the two calculated I_{PD} are identical for the actual PD location, By comparison, it is possible to find the 'K' at which two calculated I_{PD} are closer to each other, alternatively if far away it means the location position is further from the correct PD location. This 'K' shows the turn number where PD signals are originated.

3.4 Simulation and Results

To investigate the accuracy of the proposed method, a 60 discs MTL winding model is simulated in the Matlab. The PD signals, occurred at the 30th disc in this simulation, two Ipd were computed. Fig. 3.6 to Fig. 3.11 shows two computed signals assuming in 2, 10, 20, 30, 40 and 50 discs as PD origin. In 30th disc two I_{PD} are identical to each other as shown in Fig. 3.9. Hence, the PD location has been estimated correctly. It should be noted that as PD source moves away from the 30th disc to the other discs, the distance between two signals will be increased. This shows that PD localization method is consistent; therefore it is a reliable method. In disc 2, 10, and 20, the $I_{PD}1$ and $I_{PD}2$ are correlated to each other and shows similar impedance between 0 to 2 MHz as shown in Fig. 3.6, Fig. 3.7, Fig. 3.8 respectively. However, in 40th and 50th disc $I_{PD}1$ and $I_{PD}2$ are not correlated to each other as shown in Fig. 3.10 and Fig. 3.11. It is suggested that a PD pulse as an addition to the transformer will influence frequency response of forward discs.

Fig. 3.3 shows the frequency responses of the phase of Is and In at 30th disc, and also Fig. 3.4 describes the frequency responses of the phase of TFL and TFN at 30th disc.

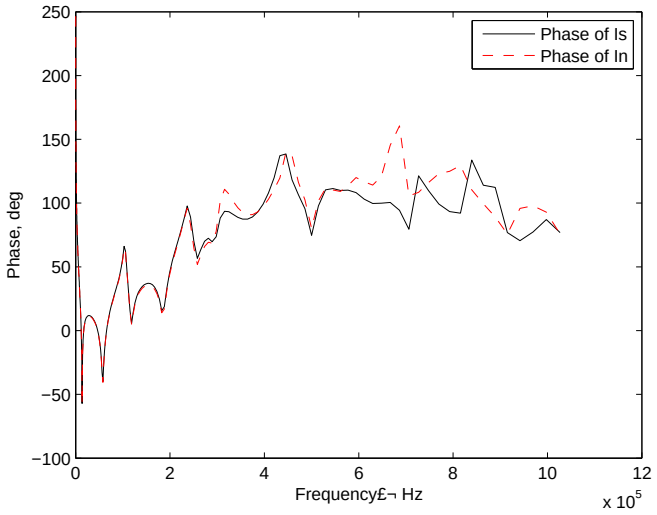

Figure 3.3: The transfer function phase frequency responses of Is and In

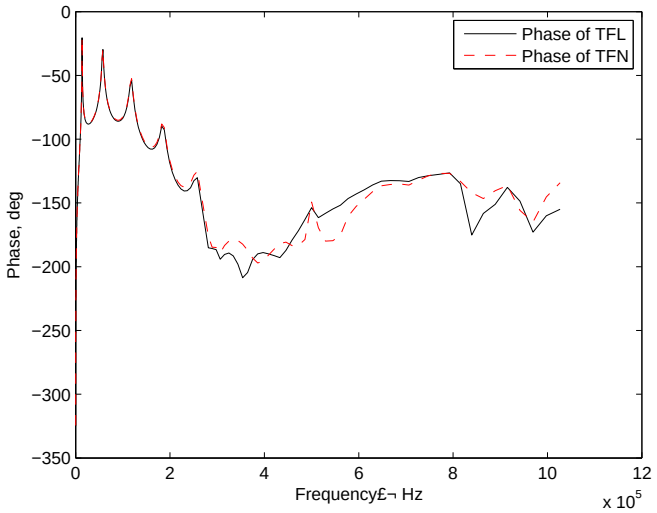

Figure 3.4: The transfer function phase frequency responses of TFL and TFN

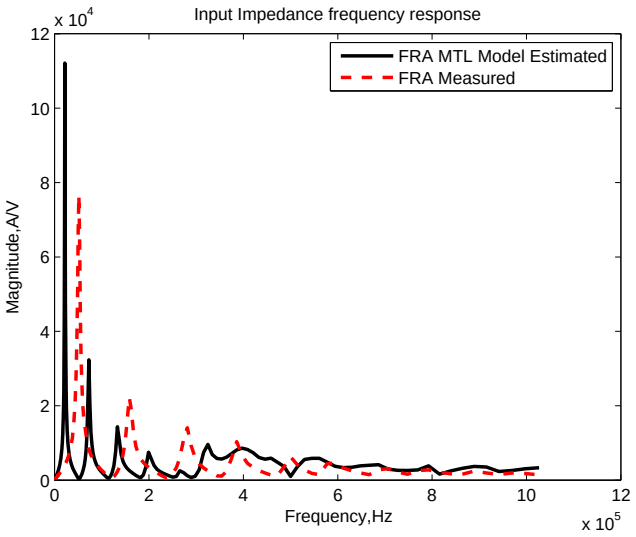

Figure 3.5: The transfer function magnitude frequency responses of input impedance

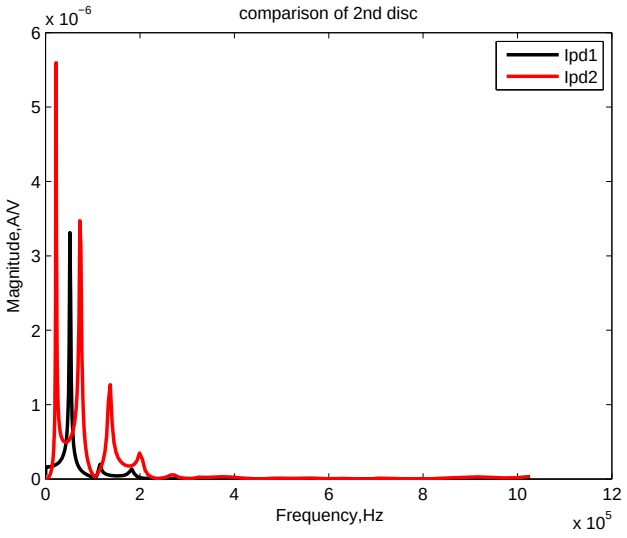

Figure 3.6: Magnitude of transfer function between $I_{PD}1$ and $I_{PD}2$ in 2nd Disc

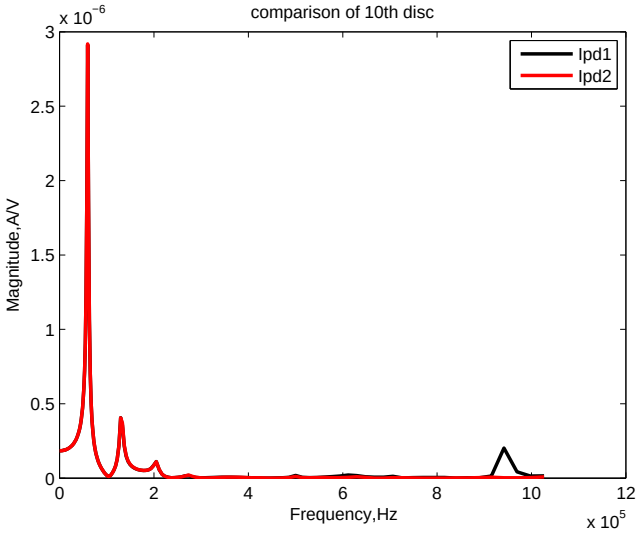

Figure 3.7: Magnitude of transfer function between $I_{PD}1$ and $I_{PD}2$ in 10th Disc

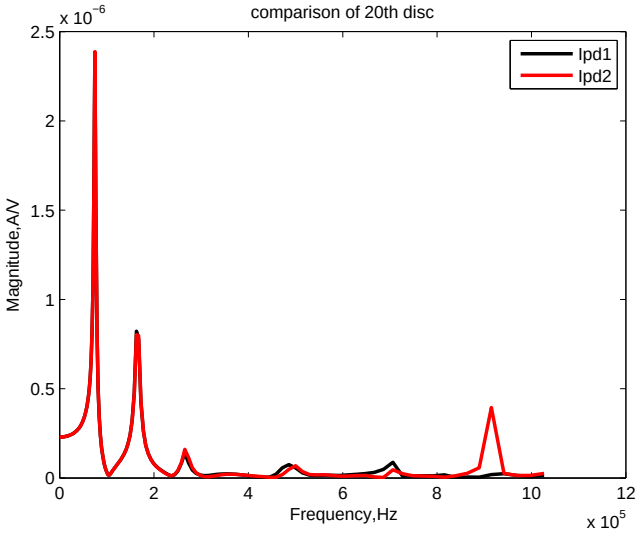

Figure 3.8: Magnitude of transfer function between $I_{PD}1$ and $I_{PD}2$ in 20th Disc

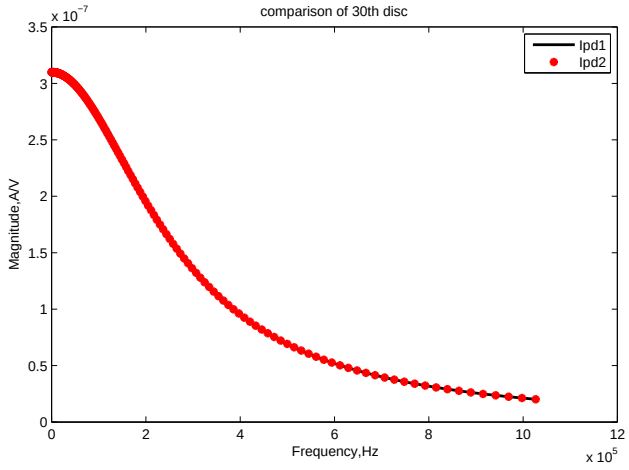

Figure 3.9: Magnitude of transfer function between $I_{PD}1$ and $I_{PD}2$ in 30th Disc

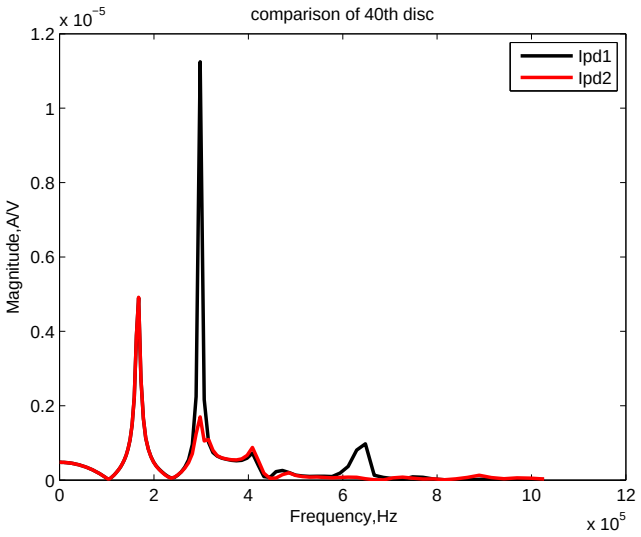

Figure 3.10: Magnitude of transfer function between $I_{PD}1$ and $I_{PD}2$ in 40th Disc

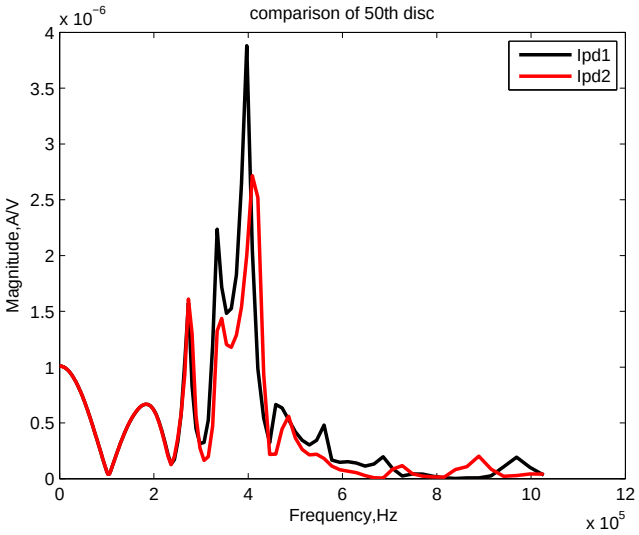

Figure 3.11: Magnitude of transfer function between $I_{PD}1$ and $I_{PD}2$ in 50th Disc

3.5 Summary

The transformer winding was simulated by the use of a multi-conductor transmission line model. In this chapter, the calculation of the MTLM formula has been illustrated. The calculation of transfer function concerning line-end and neutral-end is used to find a partial discharge location. Then two measured PD signals at both ends were referred to internal points of the winding using two calculated transfer functions. Two referred signals are closer to each other for the actual PD location.

Overall, locating partial discharge in transformers is a very difficult task due to the complexity of winding modeling in high frequencies. MTLM is one of the most suitable models for PD propagation study in transformers. The disadvantage of MTLM is that the solution is too complex and time-consuming.

Chapter 4

Lumped Parameter Winding Modelling of Power Transformers for Frequency Response Analysis

4.1 Introduction

Fast transient overvoltage can be caused by various transformer faults. Once transients occur, it may induce overvoltage at resonant frequencies in a winding, and it may cause damage to transformer insulation. To minimize the risk of excessive transient overvoltage, different transformer models are used to simulate possible transients inside a winding. The existing transient transformer models include the lumped parameter model and the multi-conductor transmission line (MTL) model. An MTL model can apply for wide-frequency range modeling, and the upper frequency range for this model is up to a few MHz. However, the analytical equation of MTL model has a large scale, because it uses a turn-to-turn modeling procedure instead of disk-to-disk modeling, and it cost a large amount of computational time.

Conventional lumped Resistor-Inductor-Capacitor (RLC) models as divide a winding into many units on coil-or turn basis, which have been suc-

cessfully used in analysing natural frequencies [1] and simulating lightning impulse transients, switching transients [35] and local oscillations in windings [1]. In a real transformer, each turn has its own parameters such as resistance, capacitance, and inductance. Once combining several turns into one electrical lumped element, these parameters are merged. An RLC model can be employed without complex computation procedures. However, the valid upper range frequency of a lumped RLC model is much less than that of an MTL model with only a few hundred kHz [36]. Another solution to simulate fast transients in large power transformer windings is a hybrid model built by a combination of a detailed model and black box models [37]. Currently, most of the frequency dependent modeling of transformers are focused on the lumped parameter model. The objective of this chapter is to develop an improved lumped model with less complexity and higher validly of frequency. For improving the valid frequency range of a lumped RLC model, the essential idea is to modify a conventional lumped RLC model and make it approach a more accurate approximation to an MTL model [8].

In this chapter, the frequency response analysis (FRA) range of the improved lumped parameter model extends to 3 MHz by adding a negative-value capacitive branch in parallel with an inductive branch [8]. The original lumped model can only be used in low frequency range analysis up to 1 MHz.

4.2 One-winding Lumped Model

One-winding model is shown in Fig. 4.1, and it has same notations as a two-winding model, but without winding affiliations. The mathematical description of the model in the frequency domain is usually given in a matrix form of nodal equations applying the first and second Kirchhoff's laws [3][4][10]

$$YU = AI; ZI = -A^T U; \tag{4.2.1}$$

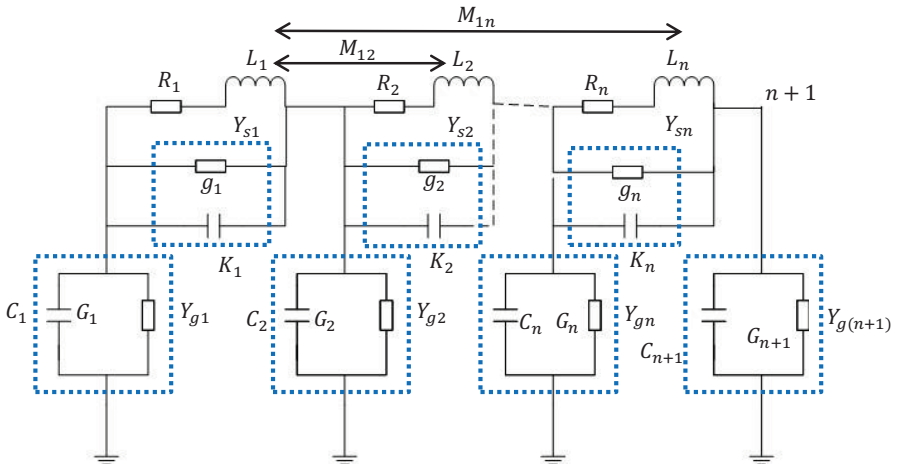

Figure 4.1: Equivalent circuit of a single-phase one-winding power transformer

where vectors U and I represent node voltages and branch currents respectively:

$$U = \begin{bmatrix} U_1 \\ U_2 \\ \dots \\ \dots \\ U_{2n+2} \end{bmatrix} \tag{4.2.2}$$

$$I = \begin{bmatrix} I_1 \\ I_2 \\ \dots \\ \dots \\ I_{2n} \end{bmatrix} \tag{4.2.3}$$

The incidence matrix A serves to link nodal voltages with branch current:

$$A = \begin{bmatrix} S & 0 \\ 0 & S \end{bmatrix} \tag{4.2.4}$$

The branch impedance matrix Z consist of the inductance matrix L and

the resistance matrix R as follow:

$$Z = j\omega L + R \tag{4.2.5}$$

Where S is a $(n+1) * n$ matrix:

$$S = \begin{bmatrix} -1 & 0 & 0 & ... & 0 & 0 \\ 1 & -1 & 0 & ... & 0 & 0 \\ 0 & 1 & -1 & ... & 0 & 0 \\ ... & ... & ... & ... & ... & ... \\ 0 & 0 & 0 & ... & 1 & -1 \\ 0 & 0 & 0 & ... & 0 & 1 \end{bmatrix} \tag{4.2.6}$$

The admittance matrix 'Y' has dimension as $(2n+2) * (2n+2)$ and each element of 'Y' is a combination of admittances 'Y_s' and 'Y_g', corresponding to series conductance 'g' and series capacitance 'K', and ground conductance 'C' and ground capacitance 'G'. The capacitance of a physical system is defined by its geometrical capacitance and the relative permittivity of the dielectric material used. In the lumped circuit model, a parallel circuit representation was used for representing these losses. The overall capacitance is composite of the geometrical capacitance 'C_geo', obtained on the basis of a physical dimension of transformer windings, and the complex effective relative permittivity of insulation $\varepsilon^{'}$ as the following [1][2]:

$$Y = j\omega\varepsilon C_{Geo} = \omega\varepsilon^{'} C_{Geo} + j\omega\varepsilon^{''} C_{Geo} = G + j\omega C \tag{4.2.7}$$

where $C = \varepsilon^{'} C_{Geo}$ and $G = \varepsilon^{''} C_{Geo}$ represent the capacitance and conductance of the parallel circuit model.

$$Y_s = sK + g \tag{4.2.8}$$

$$Y_g = sC + G \tag{4.2.9}$$

$$Z = jwL + R \tag{4.2.10}$$

$$\begin{cases} I_s = Y_g U_s + (Z^{-1} + Y_s)(U_S - U_R) \\ I_R = Y_g U_R + (Z^{-1} + Y_s)(U_R - U_s) \end{cases} \tag{4.2.11}$$

4.3 Two-port Transmission Line Model

In general, a transmission line is considered as a cascade of sections of length, each of which consists of lumped components 'R', 'L', 'C' and 'G', representing resistance, inductance, shunt capacitance and conductance per unit length of a line, respectively, as shown in Fig. 4.2. The equations of transmission line are derived on the basis of the Kirchhoff's voltage and current laws, and are known as Telegrapher's equations [5][6][7]:

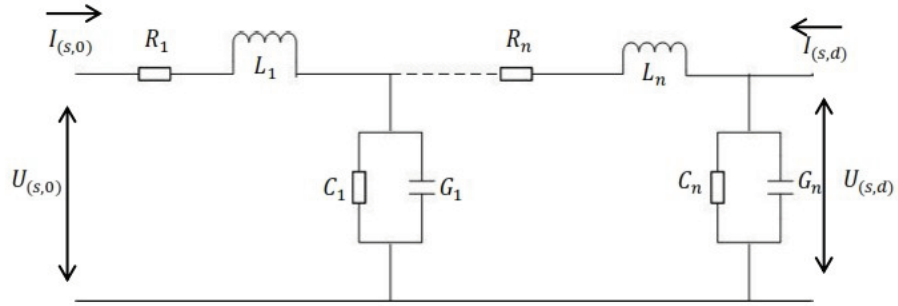

Figure 4.2: Equivalent circuit of a single-phase one-winding power transformer

$$\frac{\partial U(s,x)}{\partial x} = -SLI_{(s,x)} - rI_{(s,x)} = -ZI_{(s,x)} \tag{4.3.1}$$

$$\frac{\partial I(s,x)}{\partial x} = -SCU_{(s,x)} - GU_{(s,x)} = -YU_{(s,x)} \tag{4.3.2}$$

where $U(s,x)$ and $I(s,x)$ are the Laplace transforms of the time domain voltage $u(t,x)$ and current $i(t,x)$ respectively in the frequency domain:

$$Z = jwL + R \tag{4.3.3}$$

and

$$Y = sC + G \tag{4.3.4}$$

Consider a transmission line as a two-port network in terms of voltages and currents $U(s,0)$, $I(s,0)$ and $U(s,d)$, $I(s,d)$ at the input $(x=0)$ and output $(x=d)$ of the network respectively in the matrix form as follows [58][6]:

$$\begin{bmatrix} U_R \\ I_R \end{bmatrix} = \begin{bmatrix} \cosh(\gamma d) & -Z_c \sinh(\gamma d) \\ -{Z_c}^{-1} \sinh(\gamma d) & \cosh(\gamma d) \end{bmatrix} \begin{bmatrix} U_S \\ I_S \end{bmatrix} \tag{4.3.5}$$

An expression of two-port equations can be obtained from 4.3.3 and 4.3.4 as:

$$\begin{cases} I_S = coth(\gamma d)\, U_s - Z_c sinh(\gamma d)\, U_R \\ I_R = -{Z_c}^{-1} sinh^{-1}(\gamma d)\, U_s + cosh(\gamma d)\, I_s \end{cases} \tag{4.3.6}$$

where $\gamma = \sqrt{ZY}$ and $Z_c = \sqrt{Z/Y}$ is the impedance of the uniform transmission line. Let

$$Y_1 = Z_c \tanh\left(\frac{\gamma d}{2}\right) \tag{4.3.7}$$

$$Y_2 = Z_c sinh^{-1}(\gamma d) \tag{4.3.8}$$

and equation 4.3.6 can rewritten as

$$\{ \begin{array}{c} I_S = Y_1 U_s + Y_2 (U_s - U_R) \\ I_R = Y_1 U_R + Y_2 (U_R - U_S) \end{array} \tag{4.3.9}$$

Both equation 4.2.11 and equation 4.3.9also can present as 4.3.10

$$\begin{cases} I_s = Y_{11}U_s + Y_{12}U_R \\ I_R = Y_{12}U_s + Y_{11}U_R \end{cases} \tag{4.3.10}$$

where the coefficients for the MTL model in equation 4.3.10 $Y_{11} = Z_c coth(\gamma d)$, $Y_{12} = Z_c sinh^{-1}(\gamma d)$

4.4 Proposed Improved Lumped Parameter Model

In order to increase the valid frequency range of a lumped RLC model, the basic idea is to modify the conventional lumped RLC model to make it become more accurate approximation to the MTL model based on the following equations [8].

$$cothx = x^{(-1)} + 1/3x - 1/45x^3 + 2/945x^5 - ..... \tag{4.4.1}$$

$$sinh^{(-1)}x = x^{(-1)} - 1/6x + 7/360x^3 - 31/15120x^5 - ..... \tag{4.4.2}$$

the approximation is assumed as

$$cothx \cong x^{-1} + k_1 x \tag{4.4.3}$$

$$sinh^{-1}x \cong x^{-1} + k_2 x \tag{4.4.4}$$

Let a function $f(x) = cothx - x^{-1} \cong k_2 x$ and take 1000 samples in the range of $0 < x < j1.6$, $k_1 \cong 0.375$ and $k_2 = -0.125$ were obtain using above mathematical function. Then, the coefficient matrices Y_{11} and Y_{12} in 4.2.11 can be denoted as:

$$Y_{11} = z^{(-1)} + 3/8Y \tag{4.4.5}$$

$$Y_{12} = z^{(-1)} + 1/8Y \tag{4.4.6}$$

According to equation4.4.5 and 4.4.6, equation 4.2.11 can also be denoted as:

$$\begin{cases} I_s = \frac{1}{2}Y_g U_s + (Z^{-1} - \frac{1}{8}Y_s)(U_S - U_R) \\ I_R = \frac{1}{2}Y_g U_R + (Z^{-1} - \frac{1}{8}Y_s)(U_R - U_s) \end{cases} \tag{4.4.7}$$

As a result, the performance of a lumped model parameter can be improved by adding a negative-value capacitive branch in parallel with the inductive branch, which compensates for the decrease of the susceptance of the inductive branch with the increase of frequency as shown below:

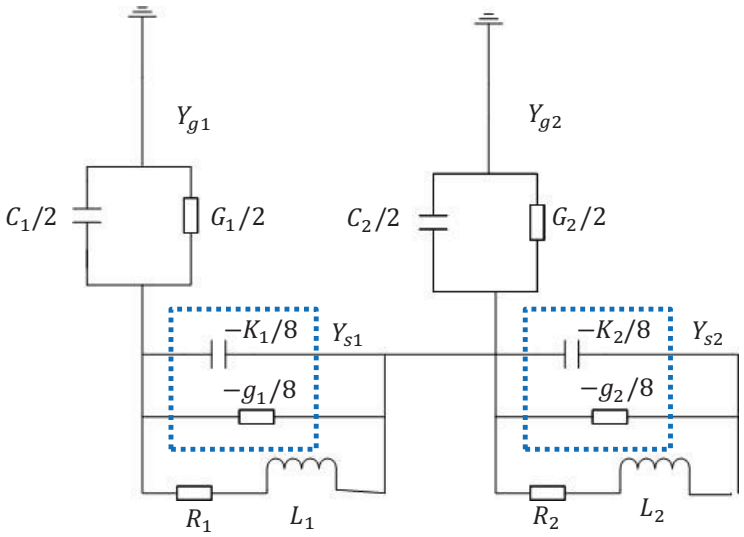

Figure 4.3: Equivalent circuit of the improved lumped model

$$\begin{bmatrix} Y_s = -\frac{1}{8}(sK + g) \\ Y_g = \frac{1}{2}(sC + G) \\ Z = j\omega L + R \end{bmatrix} \tag{4.4.8}$$

where s denotes the imaginary unit, ω is the angular frequency, and K, C, and R are series capacitance, ground capacitance, and winding resistance respec-

tively. Matrix L consists of the self- and mutual sectional inductances L and M. The overall capacitance is composite of the geometrical capacitance C_{geo}, obtained on the basis of the physical dimension of transformer windings, and the complex effective relative permittivity of insulation $\varepsilon^{'}$ as the following [1][3]:

$$C = \varepsilon^{'} C_{geo} \tag{4.4.9}$$

$$K = \varepsilon^{'} K_{geo} \tag{4.4.10}$$

In addition, the expression of the overall conductance G can be written as below [12]:

$$G = C\omega tan\delta \tag{4.4.11}$$

where $tan\delta$ is the dissipation factor, defined as the ratio between the imaginary and the real parts of the relative permittivity. The calculation of winding resistance is one of the major challenges due to the eddy current effect in a winding conductor and a core. There are many methods being proposed and utilised for the winding resistance calculation, among which, the Dowell's approach [2][10][11] is one of the most referenced:

$$R = R_{dc}\Delta \left(\frac{\sinh(2\Delta) + \sin(2\Delta)}{\cosh(2\Delta) - \cos(2\Delta)} + \frac{2(p^2 - 1)}{3} \frac{\sinh(\Delta) - \sin(\Delta)}{\cosh(\Delta) + \cos(\Delta)} \right) \tag{4.4.12}$$

where R_{dc} is the DC resistance of one winding section, p is the number of layers in the section, and Δ is defined as,

$$\Delta = \left(\frac{\pi}{4}\right)^{3/4} \frac{d^{3/2}}{\delta t^{1/2}} \tag{4.4.13}$$

in which d is the conductor equivalent diameter and t is the distance between the centers of two adjacent conductors. The skin depth can be found as follows:

Where σ and μ_r are the conductor conductivity and relative permeability respectively.

4.5 Transfer Function of Transformer Winding for Frequency Response Analysis

Frequency responses of transformer winding are determined by transfer functions of the ratio of nodal voltages and inductive branch currents with respect to the applied input voltage. The method to use FRA into simulation, assuming an external voltage source into a node k, this voltage will become an input voltage. Thus, matrices Q and P are introduced as the component vectors of the matrices Y and A[3][9][10]. After that, equation 4.2.1 and 4.2.4 can be written as:

$$YU = AI + QU_k \tag{4.5.1}$$

$$ZI = -A^T U + PU_k \tag{4.5.2}$$

where voltage U_k represents an input sinusoidal voltage signal. From the equation, the branch currents and nodal voltage vectors can be written as[3][10][57]:

$$U = ((Y + AZ^{-1}A^T)^{-1}(AZ^{-1}P + Q)U_k) \tag{4.5.3}$$

$$I = Z^{-1}(-A^T U + PU_k) \tag{4.5.4}$$

The expressions for transfer functions of winding models listed as below[3][4][10]:

$$H(s) = \frac{U_f}{I_f} = \frac{((Y + AZ^{(-1)}A^T)^{(-1)}(AZ^{(-1)}P + Q)U_k)}{(Z^{(-1)}(-A^TU + PU_k))} \tag{4.5.5}$$

4.6 Simulation Results and Comparison

In order to verify the improved lumped model, the frequency response of single-phase experiment transformer without core, with 60 discs, the number of 11 turns per disc is simulated using the developed model.

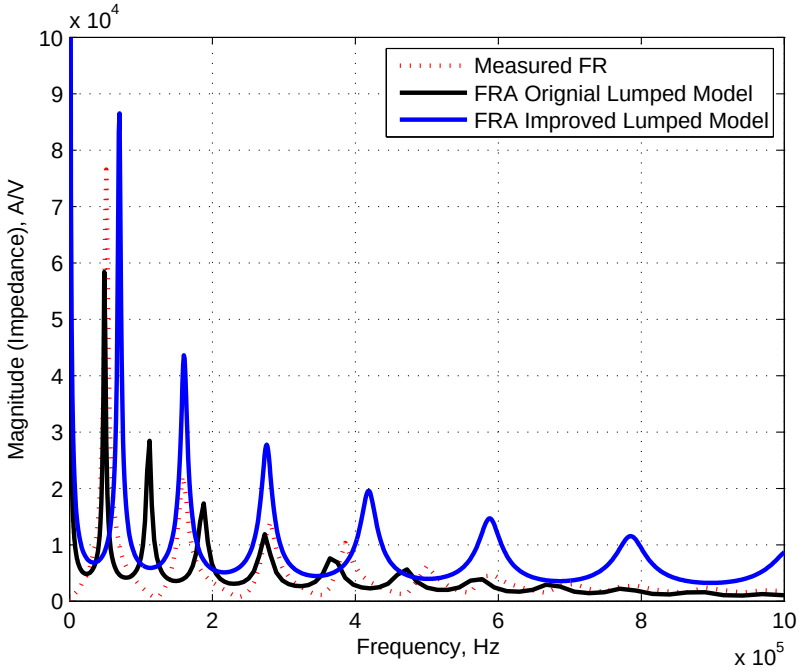

Figure 4.4: Comparison between the transfer function magnitude frequency response of original lumped model, improved lumped model and reference

Fig. 4.4 shows the frequency response analysis results. FRA of improved lumped model has positive frequency shift between 0 to 100 kHz. From 100 kHz to 400 kHz, the improved lumped model shows better performance than original model, its magnitude is much closer to measured values and there are no frequency shifts between 150 kHz to 300 kHz.

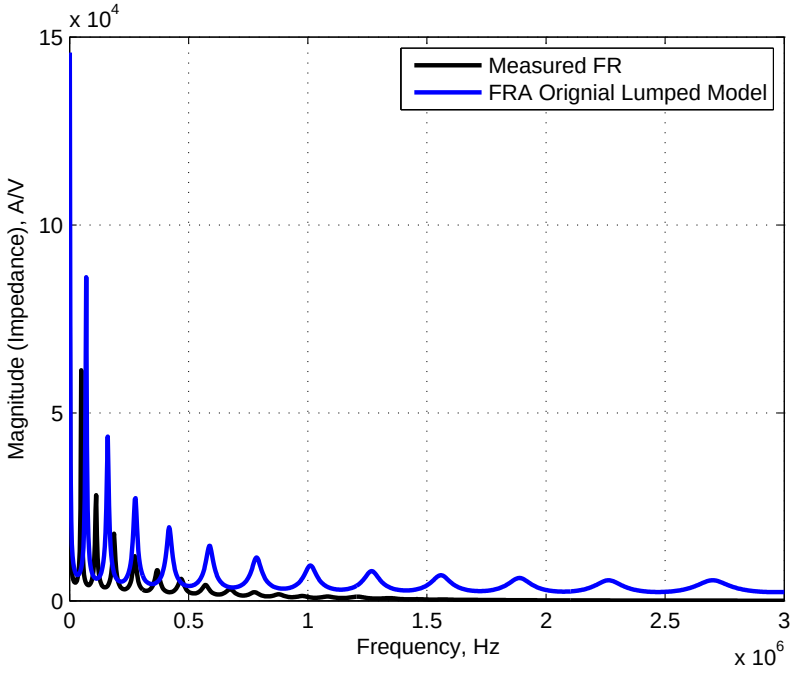

Figure 4.5: Comparison between the transfer function magnitude frequency response of original lumped model and improved lumped model

The simulation of FRA in the high frequency range gives the results of the original lumped model and improved lumped model. Fig. 4.5 clearly shows frequency responses of the original lumped model weaken after 500 kHz and impedance decrease to zero approximately around 1.5 MHz. However, the improved lumped model produces stronger frequency response up to 3MHz. In conclusion, the frequency response of the lumped model has been improved.

4.7 Summary

Fast transient phenomena in transformer windings require a wider frequency range up to several MHz. MTLM covers a wider range frequency, but it is too complex to be calculated in practice. Compared with MTL model, the lumped model requires less computation, but it is only valid up to 1 MHz. With the aim to improve the frequency range of simulation for fast transient analysis, an improved turn-based lumped RLC model is proposed in this chapter. From the mathematics of two-port expression of MTL model, the conventional lumped RLC model is modified to make it more accurate approximation to the MTL model. The lumped RLC model is improved by adding a negative-value capacitive branch in parallel with the inductive branch, which compensates for the decrease of the susceptance of the inductive branch with the increase of frequency. The simulation results show that the valid frequency range of the improved RLC model is extended up to 3 MHz for large power transformer windings.

Chapter 5

Parameter Optimisation for Improved Parameter Winding Models

5.1 Introduction

Chapter 4 describes the frequency response analysis (FRA) of the lumped winding model. Frequency response analysis of improved lumped winding model is not identical to the simulated results due to the parameters value because inductance and resistance are affected by low frequency [3][48][49]. In this chapter, parameters of the lumped winding model using FRA measurements will be optimised further by using as artificial intelligent algorithm. In order to reduce the difference between simulations of winding models and corresponding FRA measurements[52][53], three methods are employed to optimise the model parameters, i.e., Particle Swarm Optimization (PSO)[51], Genetic Algorithms (GA) [50] and Simulated annealing (SA) [56].

5.2 Particle Swarm Optimisation

Particle Swarm Optimization (PSO) was originally attributed to R.C. Eberhart and J. Kennedy in 1995[51]. Optimal algorithm is based on simulation of birds' foraging. This is called "swarm intelligence". Usually a single natural biological action may be unsuccessful, but the whole group has the ability to solve the complex problem. The application of this group active in artificial intelligence is "swarm intelligence". The particle swarm optimization was used to process continuous optimization problems, at present this has been expanded to apply to the combinatorial optimization problem.

With Genetic Algorithm, Ant colony optimization, PSO is an optimization method based on the group. By comparison, the main characteristic of PSO, first of all, each has a random speed, secondly, the individual has memory function, thirdly, the evolution of individuals mainly through cooperation and competition between each one. As an efficient optimization, PSO is used to solves the nonlinear problem, and non-deviation work and peak value optimization problem. The PSO algorithm program is simple and has less adjustable parameters. There are a variety of improvements attributed to the PSO algorithm that have been applied in many fields of science and engineering.

Particle swarm optimization is an extremely simple algorithm that seems to be effective for optimising a wide range of functions. Conceptually, it seems to lie somewhere between genetic algorithms and evolutionary programming. It is highly dependent on stochastic processes, like evolutionary programming. The adjustment toward 'pbest' and 'gbest' by the particle swarm optimizer is conceptually similar to the crossover operation utilised by genetic algorithms. It uses the concept of fitness, as do all evolutionary computation paradigms.

The Basic PSO algorithm consists of the velocity:

$$v_i(k+1) = v_i(k) + \gamma_{ii}(p_i - x_i(k)) + \gamma_{2i}(G - x_i(k)) \tag{5.2.1}$$

And position

$$x_i(k+1) = x_i(k) + v_i(k+1) \tag{5.2.2}$$

- $I \rightarrow$ particle index
- $k \rightarrow$ discrete time index
- $v \rightarrow$ velocity of ith particle
- $x \rightarrow$ position of ith particle
- $p \rightarrow$ best position found by ith particle(personal best)
- $G \rightarrow$ best position found by swarm(global best, best of personal bests)
- $\gamma^{1,2} \rightarrow$ random numbers on the interval[0,1]applied to ith particle

The common PSO Algorithm

$$v_i(k+1) = \beta(k)V_i(k) + \alpha_2[\gamma_{ii}(p_i - x_i(k))] + \alpha_2[\gamma_{2i}(G - x_i(k)) \tag{5.2.3}$$

- $\beta \rightarrow$ inertia function
- $\alpha_{1,2} \rightarrow$ acceleration constants

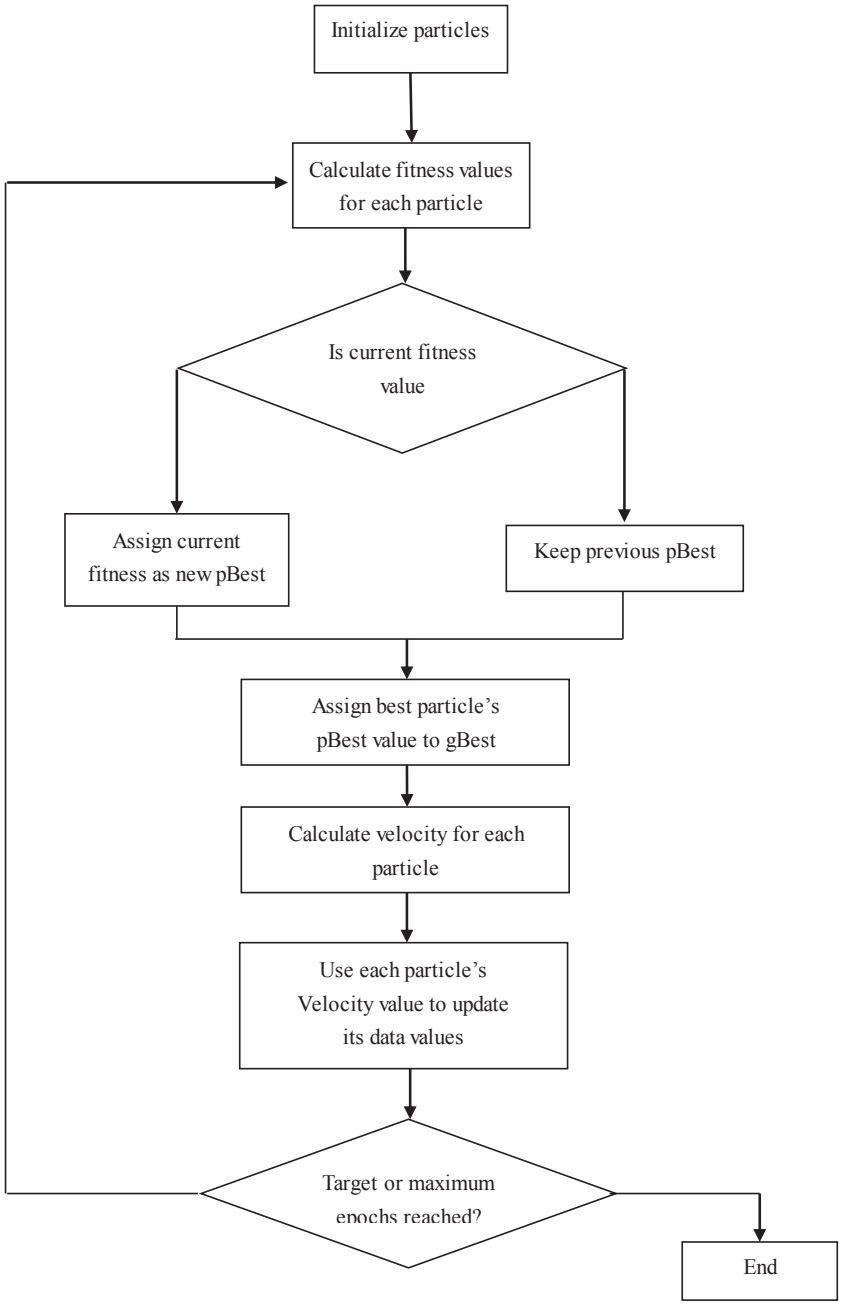

Figure 5.1: PSO Flowchart

5.3 Genetic Algorithms

Genetic Algorithms is based on the principle of biological evolution theory which is widely used, and is a highly efficient random search and optimization method. The main characteristic is the group search and information exchange between individuals, so that search strategy is not dependent on the gradient information. It was established in the early 70s established by Holland [54], and later developed by Goldberg[50]. At the beginning, genetic algorithm was not designed to be used for solving optimization problems, it was combined with evolution strategy and evolutionary programming to constitute the main framework of the evolutionary algorithm which was used for the development of artificial intelligence.

In recent years, genetic algorithm optimization has been mainly used to optimize complex problems and applications in the industrial area. It makes a contribution attracting the attention of many people. Moreover, gaps between development, evolution strategy, evolutionary programming and genetic algorithm become smaller. The application of the genetic algorithm includes job scheduling and sequencing, reliability design, vehicle routing and group technology, equipment layout and distribution, traffic problems, etc.

Characteristics of the Genetic Algorithm

a Genetic algorithm (GA) starts from a set of string searches, rather than starting with a single solution. The traditional optimization algorithm optimizes a solution from a single initial value leading easily into the local optimal solution. Starting from the string to search, the range of coverage is larger, which is better for overall optimization.

b Genetic algorithm can deal with several individuals in the group at the same time. It evaluates multiple solutions in the search space, thereby reducing the risk of being restricted to local optimal solutions, and easier to achieve parallelization.

c Genetic algorithm, is not based on deterministic rules, because it con-

siders the probability of transition rules to guide the search direction.

d Self-organising, adaptive and self-learning habits. Genetic algorithm uses the evolutionary process to organise the information obtained from searching, the fitness of the individual has a higher probability of survival and obtains stronger genetic structure to adapt to the environment, which can be used as an approximate optimal solution.

Selection Procedure

a Initialization

Select a group, or select a string or collection of individual i, $i = 1, 2, ...$ The initial population is a set of assumption's solutions. N can definitely use a range from 30 to 160, usually in a random way produce a string or collection of individual i, $i = 1, 2$, the best optimal solution will deduce by these initial assumption solution.

b Fitness-proportion selection

Based on the principle of survival of the fitness, it chooses the next generation of individuals. Set up a selection fitness standard, generation conforms to the survival of the fitness, if not will eliminate. Given the objective function f, f (i) is called the fitness of an individual i.

$$f(i) = (f(i))/(\sum {}^{M}_{(j=1)} f(j)) \tag{5.3.1}$$

For the selected 'i' for the number of the next generation of individuals, from the equation5.3.1, high fitness individuals produce the amount of next generation, low fitness individual produces less generation, or even be eliminated. Therefore, the survival offspring has the strong ability to adapt to the environment. It is clearly designed to achieve the optimal solution.

c Cross

For the selected next generation of individuals, randomly select two individuals in the same position, in accordance with the probability P of crossover, process crossover at the selected location. This process shows

the random information exchange. When produced a new individual, it can also process a single point crossover or the multipoint crossover.

d Variation Genetic algorithm

According to the principle of biological, genetic gene variants, with mutation probability P process variations of some individuals. When there is variation, variable string corresponds to an inversion, namely 1 to 0, 0 to 1. Mutation probability P agrees with minimal variation, so the smaller values of Pm defined as 0.01 to 0.2.

e Convergence to the global optimum

When the best individual achieves an objective or the fitness of the individual has reached its limit, the iteration convergence finish.

5.4 Simulated Annealing

Simulated annealing (SA) [55][56] method is used to solve the optimization problem. The principle of using the simulation material in the process of annealing and thereby achieving the lowest temperature state. A random search technique provides a global optimization method, easy to use and already being employed in many optimal design problems.

Simulated annealing method based on the physical model has two conditions; first, when the temperature is significantly higher, the configuration of the system can automatically change and also be free to move the surface of energy or allow random fluctuation. It means that it is capable of choosing the best solution automatically. Second, when the temperature decreases, movement of the surface energy is limited, and gradually concentrates in the low energy area. Each iteration is based on the current solution as the centre and then randomly generates a new adjacent solution. When the objective function value is better, current solution will be replaced.

Simulated annealing can use probability function and control parameters to determine whether to choose a new solutions. Therefore, simulated annealing can operate out of the area, through annealing optimal solution to control the speed of convergence. Following decreasing temperature, errors will become minimise, and the solution should appear more precise, once the temperature drop down to the bottom level to get the best solution to achieve convergence.

Simulated annealing has been widely applied in the “travelling salesman problem”, allocation problem, and scheduling problem, flexible manufacturing system, structure design, and medical image processing, etc.

Simulated annealing method is to set up at temperature T, build an annealing schedule, contain the initial temperature, cool the mechanism, and cool the rate and termination condition. A program sets the timing to remain at each temperature, and cooling rate, and the value of proportion of the cooling. Annealing always happens at the same temperature. The cooling process

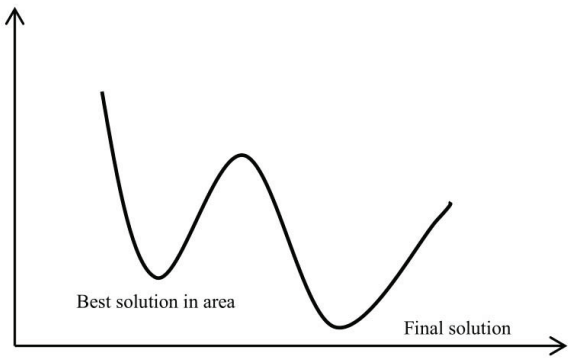

Figure 5.2: Simulated annealing function diagram

will continue in a fixed number of iterations. However, to arrive at the best solution to the problem, it requires choosing the appropriate annealing process. In addition, the simulated annealing method use Metroplis rule, which is used to decide whether to accept an energy fluctuation change, and calculation of energy E of the current solution, using the current solution as center, then randomly generated $E^{'}$, $\triangle E$=$E^{'}$-E, utility of the probability formula as below to decide whether to replace the current solution with adjacent solution:

$$P = \begin{cases} 1, if \Delta E \leq 0 \\ e^{-\frac{\Delta E}{T}}, if \Delta E > 0 \end{cases} \tag{5.4.1}$$

The basic elements of simulated annealing (SA) are the following:

1 A finite set E

2 Initial parameter, initial temperature T, ending temperature, cooling rate, the number of iterative in each temperature

3 Random generation of an initial population X, t=0

4 Centred on the current solution randomly generated new adjacent X

5 Using Metroplis rules, using a formula (1) to decide whether to replace the current solution with adjacent solution, if $X = X^{'}$,

6 Update the iterative times, t=t+1, determine whether reaching the setting iterative time, if yes, run cooling $t = 0$, two ways of cooling, firstly, $T = T = \alpha T$,$\alpha \in [0, 1]$, or $T = T - \sigma$,$\sigma < 0$.

7 Evaluate the temperature whether achieves the setting condition, if not, repeat step 3

8 Presenting the best individual in the final population as output.

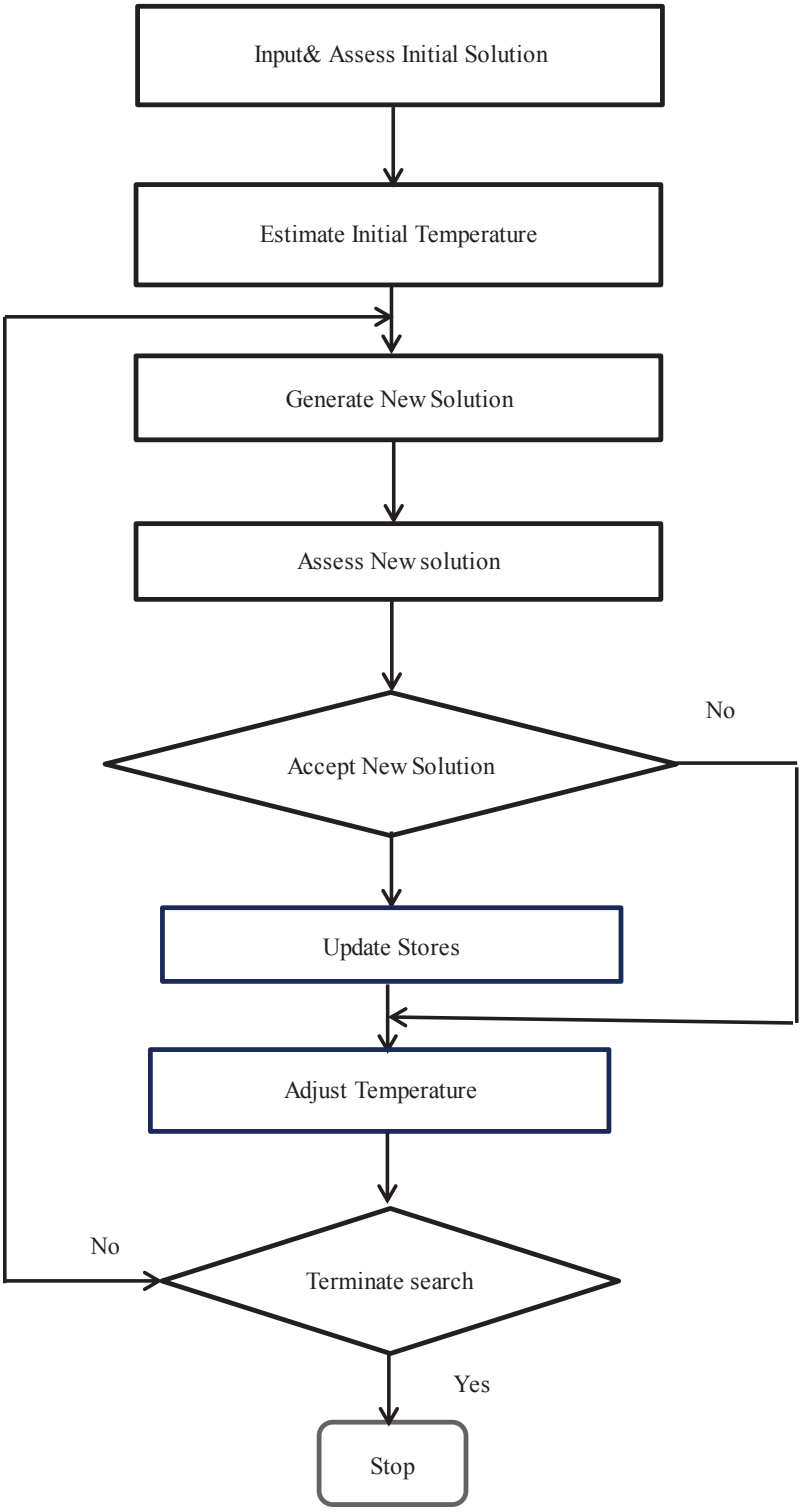

Figure 5.3: Simulated annealing flow chart

5.5 Experimental Results and Comparative analysis

In this section, parameters of lumped winding models, PSO, GA, and SA are employed to multi-parameter intelligent optimisation. Simulation studies and discussions are presented to explore the potentials of the proposed identification approach.

5.5.1 Experimental Particle Swarm Optimization Results Analysis

Identification of Local Magnetic Permeability

From the equation 4.5.5, FRA is determined by the matrix Y and Z. As can be seen in equation 4.4.8 to 4.4.13, DC resistance Rdc is used in the calculation of the frequency dependent section resistance R, thus matrix impedance Z is respect to the value of Rdc. σ and μ_r are the conductor conductivity and relative permeability will cause the change in the value of Rdc. Matrix L has influence on the Z and admittance matrix Y is determined by series capacitance and ground capacitance, K and C. Regarding the amount of parameters, K, C, σ and μ_r will effect the results of FRA. This parameters are optimised using particle swarm optimization method and then followed by FRA to analyse the effects of each parameter.

The PSO learning parameters, listed in Table 5.1, are selected on the basis of the previous study on particle swarm optimization and numerous trials with various parameter combinations using a specially written MATLAB code for PSO.

Table 5.1: PSO Parameters

Parameter	value
No of population	100
Acceleration constants, α_1	1.4962
Acceleration constants, α_2	1.4962
Inertia	0.7298

PSO learning is conducted using a set of randomly generated values of μ_r to observe the FRA. In fact, this parameter does not greatly affect the identification results as illustrated as below:

Table 5.2: Comparison between the reference and PSO identified values of local magnetic permeability

$\sigma, S/m$	Reference value	PSO Identified μ_r		Deviation from the reference
		mean	st.dev	
1×10^6	1.419×10^{-5}	1.414×10^{-5}	0.005	0.35%
2×10^6	1.419×10^{-5}	1.421×10^{-5}	0.006	0.42%
3×10^6	1.419×10^{-5}	1.412×10^{-5}	0.007	0.49%
4×10^6	1.419×10^{-5}	1.415×10^{-5}	0.004	0.28%
5×10^6	1.419×10^{-5}	1.420×10^{-5}	0.001	0.07%
6×10^6	1.419×10^{-5}	1.422×10^{-5}	0.003	0.21%
7×10^6	1.419×10^{-5}	1.416×10^{-5}	0.003	0.21%
8×10^6	1.419×10^{-5}	1.428×10^{-5}	0.009	0.63%
9×10^6	1.419×10^{-5}	1.428×10^{-5}	0.009	0.63%
10×10^6	1.419×10^{-5}	1.431×10^{-5}	0.012	0.84%

Table 5.2 summaries the reference and the parameters identified with PSO using different values of σ to analyse the effect of its in identification results. The table shows the values of μ_r and their deviations. The analysis of the table shows that the value of σ does not affect significantly the identification results in a wide range 100% from the reference value σ_{ref},where deviation of μ_r does not exceed 1% from $\mu_{r,ref}$.

Identification of Conductivity and Capacitance and Dissipation Factor

In equation 4.4.11 conductance is determined by dissipation factor $tan\delta$, hence in order to analyse the effect of dissipation factor $tan\delta_s$. The value of $tan\delta_s$is a wide range of 200% from the reference value, as shown in table 5.3, and frequency response are shown Fig. 5.4.

Table 5.3: Comparison between the reference and PSO identified Values of dissipation factor

Parameter	Reference value	PSO Identified, μ_r		Deviation from the reference
		mean	st.dev	
$tan\delta_s$	0.05	0.15	0.1	200%
$tan\delta_g$	0.05	0.15	0.1	200%

Fig. 5.4 clearly shows that the identification results are demonstrating large difference of reference when the value of $tan\delta_g$ has changed. By comparison, changing of $tan\delta_s$ has slightly effected on results. To conclude, $tan\delta_g$ has a considerable influence on the identification results.

In order to avoid the influence from other parameters, set the capacitances as identification parameters and set up σ, μ_r, tan_s and tan_g same as reference. Total number of iterations is 200.

As can be seen in Fig. 5.5, the simulation results has positive frequency shift compared to the reference frequency response within 0 to 100 kHz. However, there is no frequency shifts between 100kHz to 400 kHz. Identification results of C, K are presented in Table 5.4. The major improvement of PSO identification is an adjustment of series capacitance C to 5.6% and K to 3.5%. Fig. 5.6 shows that PSO converges down to 250. Overall, the difference between

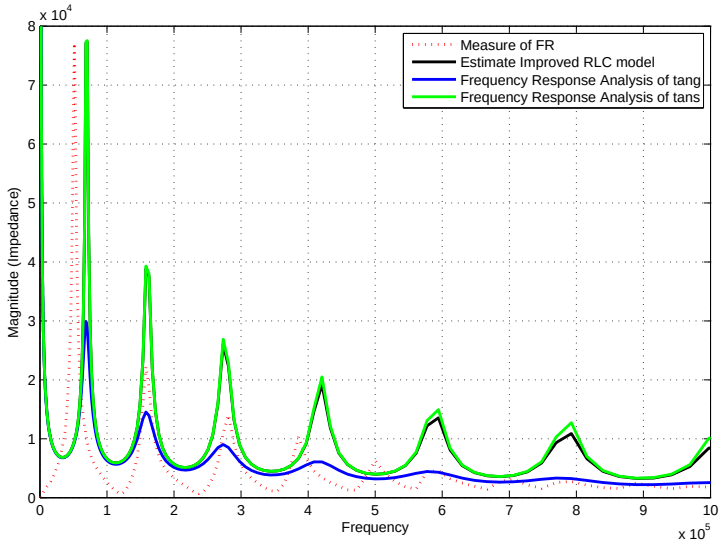

Figure 5.4: Frequency Response Analysis of $tan\delta$ from the reference value

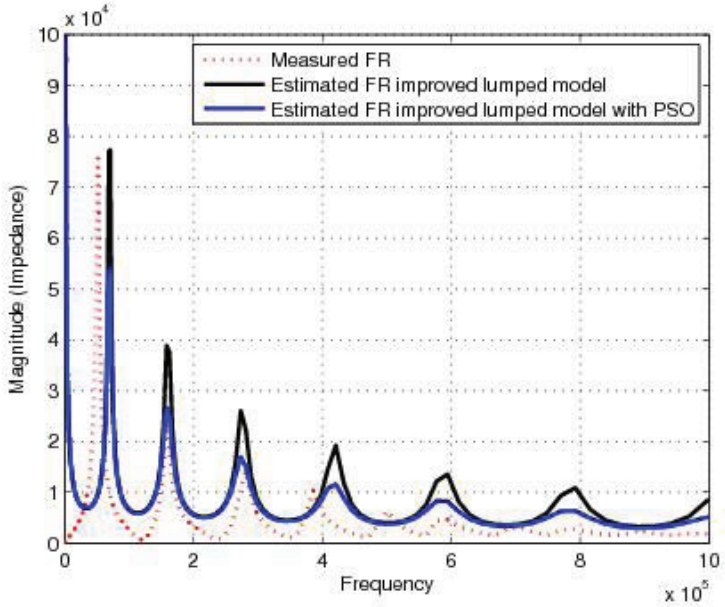

Figure 5.5: Comparison between the transfer function magnitude frequency response of improved lumped model: identified with PSO, estimated and reference

Table 5.4: Comparison between the reference and PSO identified Parameters

Parameter	Reference value	PSO Identified		Deviation from the reference
		mean	st.dev	
σ	5.8411×10^{-7}	5.8411×10^{-7}	-	-
μ_r	1.419×10^{-5}	1.419×10^{-5}	-	-
c, PF	36.339	34.299	2.04	5.6%
k, PF	116.98	112.803	4.177	3.5%
$tan\delta_s$	0.05	0.05	-	$-$%
$tan\delta_g$	0.05	0.05	-	$-$%

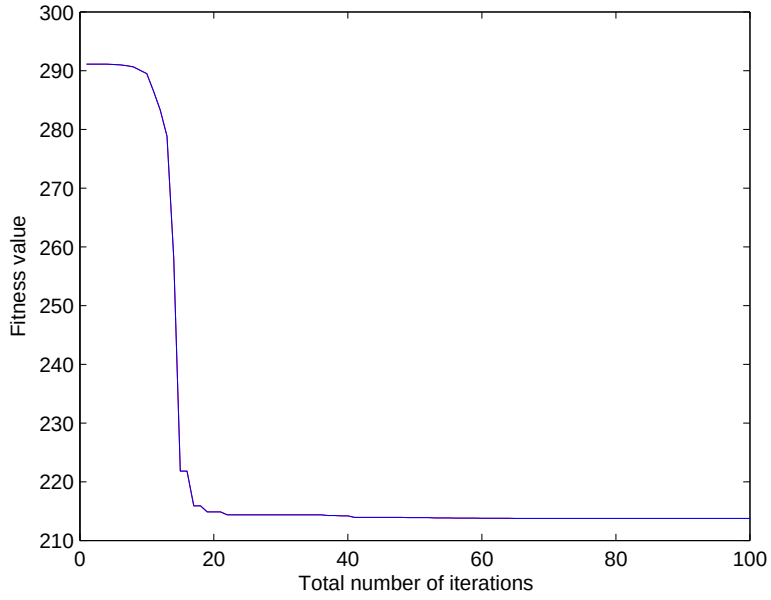

Figure 5.6: Fitness functions converges with PSO

the identified and reference parameters is negligible, it can be concluded that the identification results confirm the convergence, stability of the PSO identification process with respect to the investigated problem.

5.5.2 Experimental Genetic Algorithms Results Analysis

The wide application of Genetic algorithm is to optimise problems containing functions with multiple parameters, GA is used to optimise the main parameters, to find the best individual which can make the best solution to reach the desired value. The GA parameters are chosen based preliminary on trials using a Genetic Algorithm and Direct search toolbox for MATLAB [13]. Fig. 5.7 illustrates the comparison between measured frequency responses and estimates with the GA frequency response, where crossover operators are 0.4, and the number generated is 100.

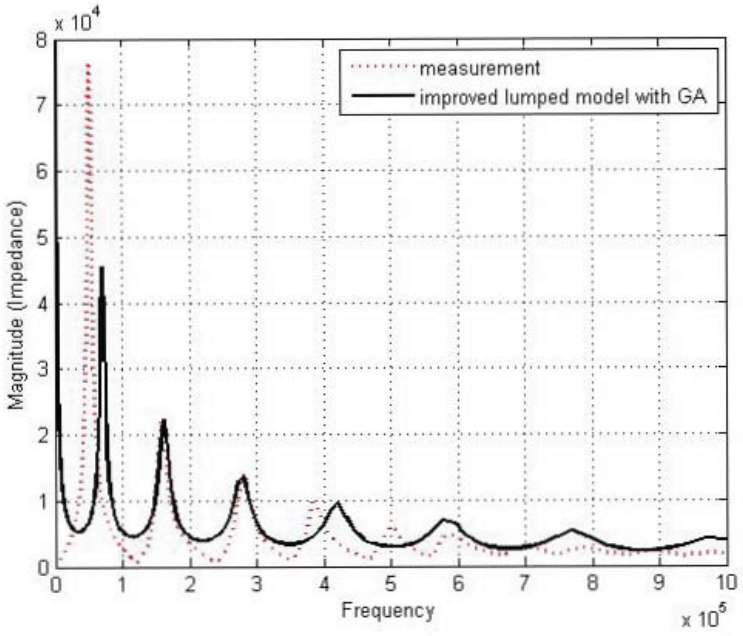

Figure 5.7: Improved lumped model frequency response with GA

Fig. 5.7 shows after genetic algorithm optimization estimated results are very similar to the measurements from 100 kHz to 300 kHz, but in the low frequency

range it still has a frequency shift. It can seem that GA was employed to decrease the magnitude slightly as well as the reference. Comparing these simulation results with measured results, it is obvious that GA identification gives closer resemblance of the frequency response with respect to the reference.

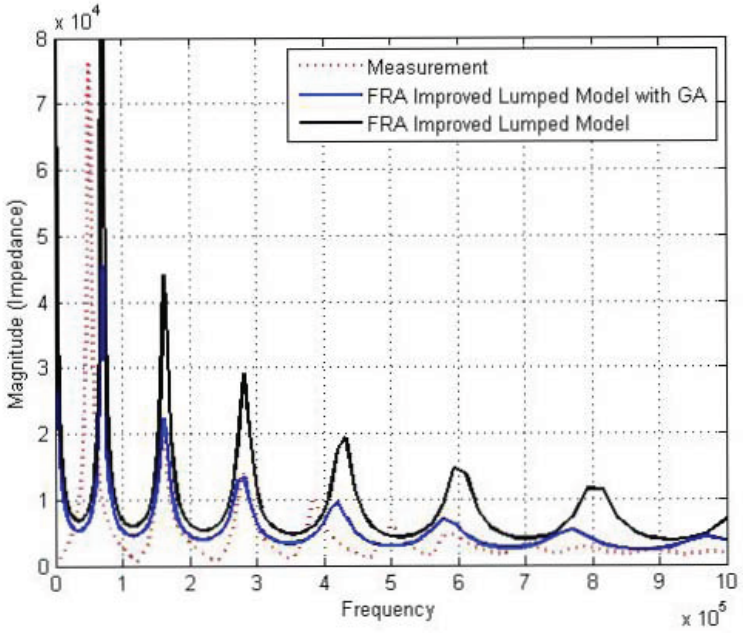

Figure 5.8: Comparison between the transfer function magnitude frequency response of improved lumped model: identified with GA, estimated and reference

As seen from the Fig 5.8, there are observed shifts in resonant frequencies after GA optimization, which primarily concern series capacitance K, DC resistance R_dc and insulation characteristics tans and tang respectively. The above parameters are optimised using the proposed parameter identification approach with GA.

Table 5.5 indicates the deviation of ground capacitance C with 26.67%. In addition, the effectiveness of insulation characteristics tans and tang also play a considerable role in this optimisation, deviation is 34% and 50.4% respectively.

Fig. 5.9 shows the fitness value decreased from 186.5 to 184 in total number of iterations of 100.

Table 5.5: Comparison between the reference and GA identified parameters

Parameter	Value of Parameter and Deviation		
	Estimated Value	GA Identified	Deviation from the reference
C,pF	36.339	46.031	26.67%
K,pF	116.98	115.38	1.36%
tans	0.05	0.067	34%
tang	0.05	0.075	50.4%

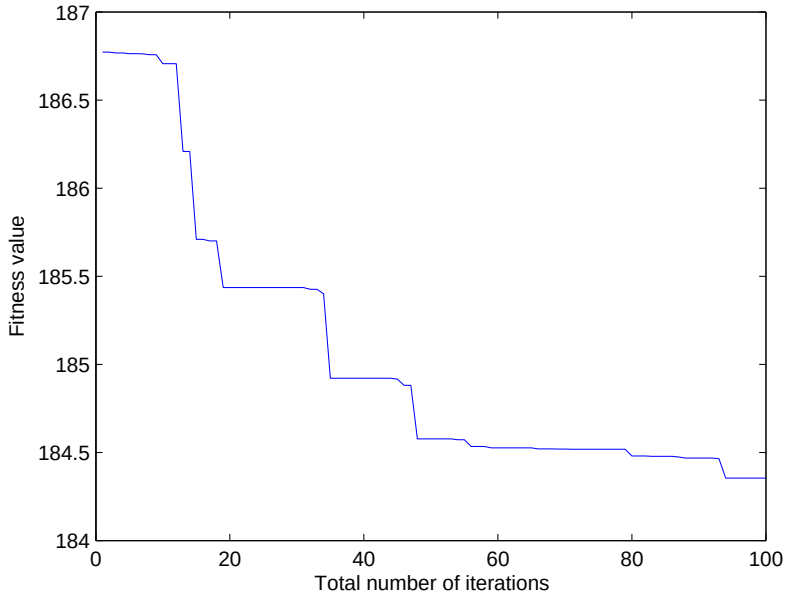

Figure 5.9: Fitness function convergence with GA

5.5.3 Experimental Simulated Annealing Results Analysis

In order to analyse the identification accuracy, three algorithms (GA, PSO, SA) are used to identify the improved lumped winding model based on the FRA. The original initial value and the identified value by SA are presented in Table 5.6, which show the deviation from the reference of C, K, tans, and tang is 129.5%, 80%, 81%, 90%, respectively.

Table 5.6: Comparison between the reference and identified parameters

Parameter	Value of Parameter and Deviation		
	Original Value	SA Identified	Deviation
C,pF	36.339	83.415	129.5%
K,pF	116.98	22.244	80%
tans	0.05	0.0095	81%
tang	0.05	0.0949	90%

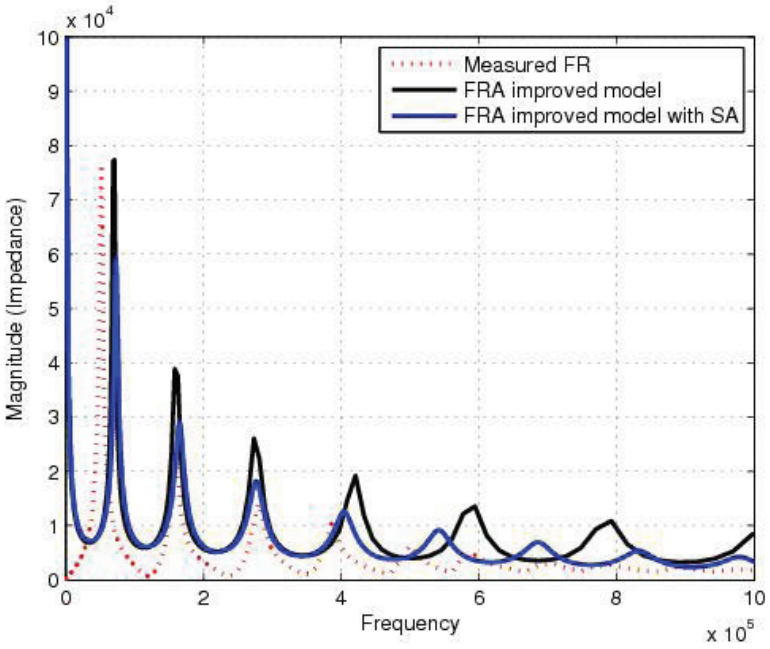

Figure 5.10: Comparison between the transfer function magnitude frequency response of improved lumped model: identified with SA, estimated and reference

Fig. 5.10 shows that SA optimization estimated results are very similar to the measurements, but it still has a frequency shift in the low frequency range similar to results from GA and PSO. Fig. 5.11 showing that the fitness value decreases from 317 to 305 in the first of 200 iterations. The fitness values has not changed between 200 to 1400 iterations. In the period of 1400 to 1500 iterations, the fitness value drops from 305 to 291. In general, SA costs more computation time on convergence and final fitness value reached at 291 in the total number of iterations of 1500.

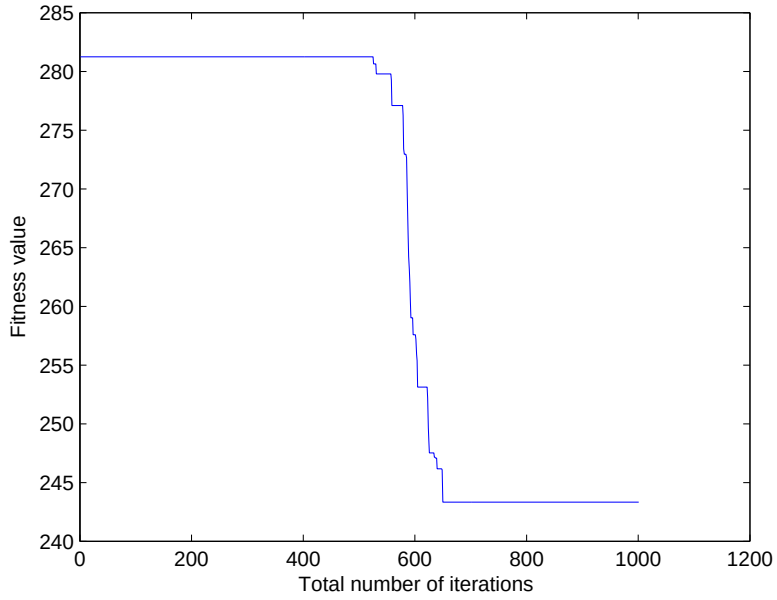

Figure 5.11: Fitness function convergence with SA

5.5.4 Comparison Results and Analysis

Identification of parameters of the lumped parameter model are presented for PSO, GA and SA learning, respectively. The initial search space for identification of the model parameters is established based on estimated parameter values. The visual comparison of Fig. 5.12 shows that the simulated magnitude of the frequency response with GA is closest to the reference. Results of PSO and SA is similar, while the magnitude of the PSO is closer to reference than the SA.

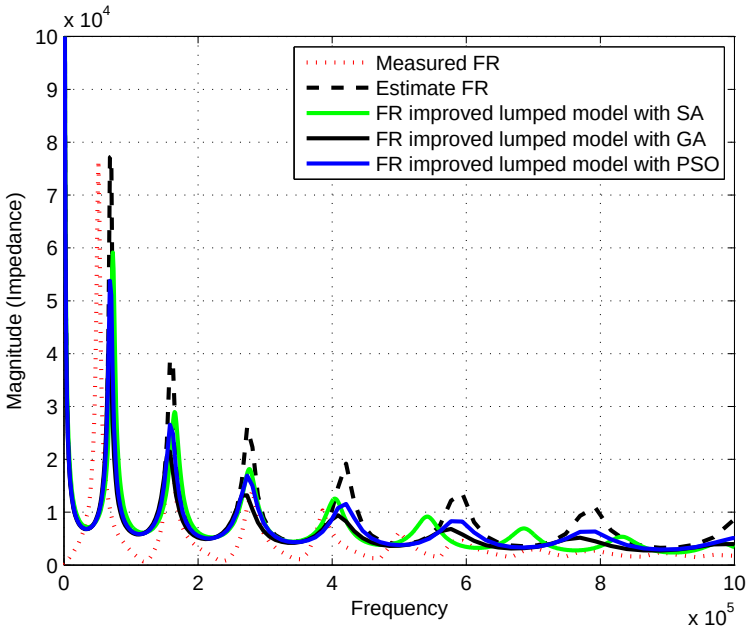

Figure 5.12: Comparison between the transfer function magnitude frequency response of improved lumped model: identified with PSO, GA, and SA, estimated and reference

Fig. 5.13 illustrates the fitness convergence of the PSO, GA and SA. The total number of iterations for PSO and GA is 100. The number of iterations of SA is 1000. Fig. 5.13 shows that the fitness value of PSO is higher than others and the fitness value of GA is less than 200. However, PSO converges faster than others which decreases from 290 to 218. The fitness value of SA stays at 282 in the first of 500 iterations, then decreases significantly between 500 iterations to 600 iterations, finally reaches at 240. The final value of fitness of SA, GA, SA is 240, 218, and

184, respectively.

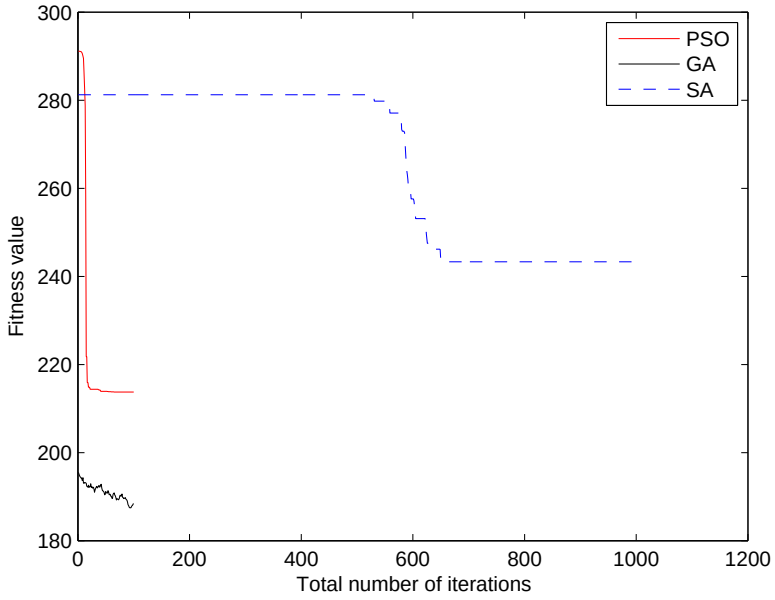

Figure 5.13: Fitness functions convergence

Table 5.4 and Table 5.6 shows that GA gives an estimate of ground capacitance C with 26.675% deviation compared with the one identified with PSO (5.6%). However, capacitance C in SA is significantly higher at 129.5%. On the contrary, GA performs better in identification of series' capacitance K with only 1.36% deviation against 3.5% deviation with PSO, the value from SA reach as 80%. Analysis of standard deviations shows that PSO is slightly superior than GA in terms of the result closeness not exceeding 5%, all deviations of each parameter of SA are higher than 80%.

Overall, SA consumes more calculation time on total processing. The identified parameters has large deviations with reference. In this case, it cannot provide a satisfactory result. The advantage of the PSO is that it has faster converge rate and smaller deviation from the reference. It may give more accurate results after the high number of iterations. In summary, considering accuracy of parameter identification, it can be concluded that GA is the most efficient for the given optimisation case.

5.6 Summary

A detailed introduction of the three optimisation methods, including particle swarm optimisation, genetic algorithms, and simulated annealing are given. They have been applied to identify the parameters of the improved lumped parameter winding modes. The simulation results show that they can determine the accurate parameters by using the reference value, and that the deviation is acceptable. The comparison of results from the optimisation methods shows that converge time of PSO is shorter than others' and the GA provides the best FRA outputs, which is closer to the reference by using a limited number of iterations.

Chapter 6

Conclusions and Future work

6.1 Conclusion

The focus of the research presented in this dissertation is to investigate ontology based diagnosis methods of power transformer faults, and power transformer winding mode by using optimisation method. Different type of power transformer failure models, diagnosis methods, ontology methods, frequency response analysis (FRA), simulation of Multi-conductor transmission line winding model (MTL) and lumped winding models have been described in this thesis.

MTL is one of the most suitable models for PD propagation study in transformers. The frequency range of this model is up to a higher frequency than the other models and usually reaches several MHz. In this study, the transfer function from all possible PD location to line-end and neutral-end were calculated. Two measured PD signals at both ends were compared with referred signals and they are closer to each other for the actual PD location. 60 discs MTL power transformer winding model has been used to justify this method. When partial discharge source occurred in the 30th disc, two referred signals are closed to each other, that confirms MTL models works effectively.

A lumped parameter model of a transformer core has been established on the basis of the duality principle between magnetic and electrical circuits. In practise, the original lumped parameter model only can be used in the low frequency range

analytically up to 1 MHz. Frequency response of a lumped model can be extended up to 3 MHz by adding a negative-value capacitive branch in parallel with an inductive branch in the original model.

A detailed introduction of the three optimisation methods, particle swarm optimisation, genetic algorithms, and simulated annealing have been given, which reveals their advantages as very powerful tools for solving multi-variables and nonlinear problems. These algorithms have been subsequently applied for transformer parameters identification based on frequency response analysis (FRA) measurements. The simulation results show that three methods can accurately identify the parameters, practical deviation between simulation with reference is acceptable. The model with the optimised parameters ideally describes the magnetic and electrical characteristics of the given transformer. The comparison of results from the optimisation methods shows that converge time of PSO is shorter than others' and the GA can provides the best FRA outputs, which are closer to the reference in a limited number of iterations.

6.2 Suggestions for Future Research

Further research may be undertaken in the following directions:

1. In this thesis, the ontology concept has been only utilised for electrical failure modes of transformer failure mode. In the future, research can be extended to other transformer failure such as mechanical deformation failure model, partial discharge failure mode.

2. The computations of MTLM are too complex and time-consuming. To decrease computational complexity two methods may be employed. The first method is to model several turns as a transmission line. The second method is to use homogenous and lossless assumption for winding insulation, which will result in simplified model equations.

3. Simulation frequency responses have been carried out at the single phase improved lumped model. Therefore, a further study will test the three-phase

power transformer.

References

[1] E. Bjerkan, "High Frequency Modeling of Power Transformers," *Ph.D. dissertation, Norwegian University of Science and Technology, Trondhiem*, 2005.

[2] P. J. Dowell, "Effects of eddy currents in transformer windings," *Electrical Engineers, Proceedings of the Institution of*, 113(8), pp. 1387-1394. 1966

[3] K. G. N. B. Abeywickrama, Y. V. Serdyuk and S. M. Gubanski, "Exploring possibilities for characterization of power transformer insulation by frequency response analysis (FRA)," *Power Delivery, IEEE Transactions on*, vol. 21, pp. 1375-1382, 2006.

[4] E. Rahimpour, J.Christian, and K. Feser, "Transfer Function Method to Diagnose Axial Displacement and Radial Deformation of Transformer winding," *power delivery, IEEE transactions on*, 18(2):493-505, 2003.

[5] L. V. Bewley, "Traveling Waves on Transmission Systems," *American Institute of Electrical Engineers, Transactions of the,* vol. 50, pp. 532-550, 1931.

[6] M. S. Ghausi and J. J. Kelly, "Introduction to Distributed-Parameter Networks With Application to Integrated Circuits," Holt, Rinehart and Winston, Inc., 1968.

[7] C. Christopoulos. "The Transmission-Line Modeling Method in Electromagnetics," Morgan and Claypool Publishers, 2006.

[8] Y. Yang, Z-J. Wang, X. Cai and Z. D. Wang, "Improved Lumped parameter model for transformer fast transient simulations," *Electric Power Applications, IET*, vol. 5, pp. 479-485, 2011.

[9] N.Abeywickrama, "Effect of Dielectric and Magnetic Material Chracteristics on Frequency reponse of Power Transformers," *Ph.D. dissertation, Chalmers University of Technology*, 2007.

[10] M. Florkowshi and J. Furgal. "Detection of Transformer Winding Deformations Based on the Transfer Function- Measurements and Simulation," *Measurement Science and Technology*, 14(11): 1986-1992, 2003.

[11] S. K. Sahoo and L. Satish, "Discriminating Changes Introduced in the Model for the Winding of a Transformer Based on Measurements," *Electric Power system Research*, 77(7): 851-858, 2006

[12] M. Popov, L.van der sluis, R. P. P. Smeets, and J. L. Rolldan. "Analysis of very Fast Transients in Layer-Type Transformer Windings," *Power Delivery, IEEE Transactions on*, vol.22, pp.238-247,2007.

[13] *Genetic Algorithm and Direct Search Toolbox User Guide for use with MATLAB*. The Math works, Inc., second edition, 2005.

[14] W. H. Tang. "Intelligent Condition Monitoring and Assessment for Power Transformers," PhD thesis, The university of Liverpool, U.K.,2004.

[15] C. Bentsson, "Status and Trends in Transformer Monitoring," *IEEE Transactions on Power Delivery*, vol. 11, pp. 1379-1384, 1996.

[16] M. Wang and K. D. Srivastava. "Review of Condition Assessment of Power Transformers in Service," *IEEE Electrical Insulation Magazine*, vol. 18, pp.12-25, 2002.

[17] N. Ding, J. Xu, Y. X. Yao, G. Wegner, I. Lieberwirth, and C. H. Chen, "Improvement of cyclability of Si as anode for Li-ion batteries," J Power Sources 192(2):644-651. doi:10.1016/j.jpowsour.2009.03.017

[18] N. A. Muhamad, B. T. Phung, T. R. Blackburn and K. X. Lai,"Comparative Study and Analysis of DGA Methods for Transformer Mineral Oil," *in Power Tech, 2007 IEEE Lausanne,*2007, pp. 45-50

[19] R. R. Rogers,"IEEE and IEC Codes to Interpret Incipient Faults in Transformers, Using Gas in Oil Analysis," *Electrical Insulation, IEEE Transactions on*, vol. EI-13, pp. 349-354, 1978.

[20] E. Dornerburg, W. Strittmatter, "Monitoring Oil Cooling Transformers by Gas Analysis," *Brown Boveri Review*, 61, pp 238-247, May 1974.

[21] S. N. Hettiwatte and H. A. Fonseka, "Analysis and interpretation of dissolved gases in transformer oil: A case study," in *Condition Monitoring and Diagnosis (CMD), 2012 International Conference on*, 2012, pp. 35-38.

[22] A. M. Emsley, and G. C. Stevens, "Review of chemical indicators of degradation of cellulosic electrical paper insulation in oil-filled transformers," *Science, Measurement and Technology, IEE Proceedings*, vol. 141, pp. 324-334, 1994.

[23] H. Monsef, A. M. Ranibar and S. Jadid, "Fuzzy rule-based expert system for power system fault diagnosis," In *Generation, Transmission and Distribution, IEE Proceedings*, vol. 144, pp. 186-192, 1997.

[24] C. P. Benjamin, P. C. Menzel, J. R. Mayer, T. M. Futrell, S. Paula, and M. Lingineni, "IDEF5 Method Report," *Knowledge based systems*, September 21, 1994

[25] T. Gruber, L. Liu, and ÖzsuM.M.Tamer, "Ontology".In the *Encyclopedia of Database Systems*, Springer-Verlag, 2009.

[26] F. Baader, D. Calvanes, D. L. McGuniness, D. Nardi, and P. F. Patel-Schineider, "The Description Logic handbook," *theory, implementation and application*, Cambridge University Press editors.2002.

[27] T. R. Gruber, "Toward principles for the design of ontologies used for knowledge sharing", *J. Human-Computer Studies*, pp.907-928, November 1995.

[28] T. R. Gruber and R. Thomas, "A Translation Approach to Portable Ontolgoy Specifications," *Knowledge Acquisition*, 5(2),199-200

[29] M. Wooldridge and N.R.Jennings.*Inteilligent Agents-Theories, Architectures, and Languages*, ISBN 3-540-58855-8.1995.

[30] P. Norvig and S. J. Russell. *Artificial IntelligenceA Modern Approach* Third edition, 2003.

[31] P. G. Baker, C. A. Goble, S. Bechhofer, N.W. Paton, R. Stevens, and A. Brass. "An Ontology for Bioinformatics Applications," *Bioinformatics*, 15(6):510-520, 1999.

[32] J. Q. Feng, Q. H. Wu, and J. Fitch. "An ontology for knowledge representation in power systems," In *Proc. of IEE Control 2004*. University of Bath, UK, September 2004.

[33] IEC Publication 60599, Interpretation of the analysis of gases in transformer and other oil med electrical equipment in &, Geneva, Switzerland, 1999.

[34] I. Boldea, "The electric generators handbook: variable speed generators," *PLondon: CRC/Taylor and Francis*, 2006.

[35] S. Tenbohlen and S. A. Ryder, "Making Frequency Response Analysis Measurements: A Comparison of the Swept Frequency and Low Voltage Impulse Methods," In *13th International Symposium on High Voltage Engineering, Netherlands*, 2003.

[36] A. Shintemirov, W.H. Tang, Q.H. Wu, "A hybrid winding model of disc-type power transformers for frequency response analysis," *Power Delivery, IEEE Transactions on*, vol. 24, pp. 730-739, 2009.

[37] G. B. Gharephpetian, H. Mohseni, and K. Moller, "Hybrid modeling of inhomogeneous transformer windings for very fast transient overvoltage studies," *Power Delivery, IEEE Transactions on*, vol. 13, pp. 157-163, 1998.

[38] Ping Zhang, You-hua Wang, Xin-peng Nie, Wei-li Yan and Hai-jiao Zhang, "A modeling for transformer windings under very fast transient over-voltages," in

Electrical Machines and Systems, 2008. ICEMS 2008. International Conference on, 2008, pp. 4309-4312.

[39] Chun. Zhao, Jiangjun. Ruan, "Frequency Effect on Calculation for voltage Distribution of Winding," *in Power & Energy Society General Meeting, 2009. PES '09. IEEE*, 2009, pp. 1-5.

[40] Ali. Mazhab. Jafari, and Asghar Akbrai, "Partial discharge location in transformer windings using multi-conductor transmission line model," *Electric Power System Research*, pp. 1028-1037September. 2007.

[41] S. N. Hettiwatte, and P.A.Crossley, "Simulation of a Transformer winding for Parial Discharge Propagation Studies," *MIEEE* ,2002

[42] M. Popov, L. Van der Sluis, G. C. Paap and H. De Herdt, "Computation of very fast transient overvoltages in transformer windings," *Power Delivery, IEEE Transactions on*, vol. 18, pp. 1268-1274, 2003.

[43] Partial Discharge Measurements, IEC standard 60270-99, 1999

[44] P. Werle, A. Akbari, H. Borsi, and E. Gockenbach, "An enhanced system for partial discharge diagnosis on power transformer," In *Proceedings of the 13th International Symposium on High Voltage Engineering*, Rotterdam, Netherlands, 2003.

[45] M. A. Elborki, P. A. Crossley, Z. D. Wang, A. Darwin, and G. Edwards, "Detection and characterization of partial discharges in transformer defect models," in *Power Engineering Society Summer Meeting, 2002 IEEE*, 2002, pp. 405-410 vol.1.

[46] S. N. Hettiwatte, P. A. Crossley, Z. D. Wang, A. Darwin, and G. Edwards, "Simulation of a transformer winding for partial discharge propagation studies," in *Proceedings of the IEEE Power Engineering Society Winter Meeting*, 2, (2002), 1394-1399.

[47] S. N. Hettiwatte, Z. D. Wang, P. A. Crossley, A. Darwin, and G. Edwards, "Experimental investigation into the propagation of partial discharge pulses in transformers," in *Power Engineering Society Winter Meeting, 2002. IEEE*, 2002, pp. 1372-1377 vol.2.

[48] S. P. Ang, J. Li, Z. Wang, and P. Jarman, "FRA Low Frequency Characteristics Study Using Duality Transformer Core Modeling," In *Proceeding of the 2008 IEEE International Conference on Condition Monitoring and Diagnostics*, pages 889-893, Beijing, China, 2008.

[49] N. Abeywickrama, A. D. Podoltsev, Y. V. Serdyuk, and S. M. Gubanski. "High-Frequency Modeling of Power Transformers for Use in Frequency Response Analysis," *IEEE Transactions on Power Delivery*, 23(4):2042-2049,2008.

[50] D. E. Goldberg, *Genetic Algorithms in search, optimisation, and Machine Learning*, Addison-Wesley Longman, Inc.,1989.

[51] J. Kennedy and R. C. Eberhart, *Swarm Intelligence*, Morgan Kaufmann Publishers, 2001.

[52] W. H. Tang, S. He, Q. H. Wu, and Z. J. Richardson, "Winding Deformation Identification Using A Particle Swarm Optimiser with Passive Congeregation for Power Transformers," International Journal of Innovations in Energy Systems and Power, 1(1), 2006.

[53] V. Rashtchi, E. Rahimpour, and E. M. Rezapour. "Using a Genetic Algorithm for Parameter Identification of Transformer R-L-C-M Model, "Electrical Engineering," 88(5):417-422, 2006.

[54] J. H. Holland, "Adaptation in Natural and Artificial Systems", An Introductory Analysis with Applications to Biology, Control, and Artificial Intelligence, MIT Press, Cambridge, Massachusetts, London, England, 1992.

[55] *Simulated Annealing, Bootstrap Matlab Toolbox*, http://www.mathworks.co.uk/discovery/simulated-annealing.html.

[56] Franco. Busetti, "Simulated annealing overview," 2003.

[57] E. Rahimpour, J. Christian, K.Feser, and H.Mohseni. "Modellierung der Transformatorwicklung zur Berechnung der Übertragungsfunktion für die Diagnose von Transformatoren", *ELEKTRIE*, 54(1):18-30, 2000.

[58] C. R. Paul, *Analysis of Multiconducotr Transmission Lines*, John Wiley &Sons, Inc., New York, 1994.